International Geology Review

Diamonds and Their Mineral Inclusions, and What They Tell Us: A Detailed "Pull-Apart" of a Diamondiferous Eclogite

Lawrence A. Taylor [a], Randall A. Keller [a], Gregory A. Snyder [a],
Wuyi Wang [a], William D. Carlson [b], Erik H. Hauri [c], Tom Mccandless
[d], Kuk-Rak Kim [e], Nikolai V. Sobolev [f] & Sergei M. Bezborodov [g]

[a] Planetary Geosciences Institute, Department of Geological
Sciences, University of Tennessee, Knoxville, Tennessee, 37996

[b] Department of Geological Sciences, University of Texas, Austin,
Texas, 78712

[c] Department of Terrestrial Magnetism, Carnegie Institution of
Washington, Washington, District of Columbia, 20015

[d] Department of Geosciences, University of Arizona, Tucson,
Arizona, 85721

[e] Institute of Geoscience, University of Tsukuba, Tsukuba, Ibaraki,
305, Japan

[f] Institute of Mineralogy and Petrography, Russian Academy of
Sciences, Novosibirsk, 630090, Russia

[g] ALROSA Co. Ltd., Mirny 678170, Sakha Republic (Yakutia), Russia

Available online: 06 Jul 2010

PLEASE SCROLL DOWN FOR ARTICLE

Diamonds and Their Mineral Inclusions, and What They Tell Us: A Detailed "Pull-Apart" of a Diamondiferous Eclogite

LAWRENCE A. TAYLOR, RANDALL A. KELLER, GREGORY A. SNYDER, WUYI WANG,

Planetary Geosciences Institute, Department of Geological Sciences, University of Tennessee, Knoxville, Tennessee 37996

WILLIAM D. CARLSON,

Department of Geological Sciences, University of Texas, Austin, Texas 78712

ERIK H. HAURI,

Department of Terrestrial Magnetism, Carnegie Institution of Washington, Washington, District of Columbia 20015

TOM MCCANDLESS,

Department of Geosciences, University of Arizona, Tucson, Arizona 85721

KUK-RAK KIM,

Institute of Geoscience, University of Tsukuba, Tsukuba, Ibaraki 305, Japan

NIKOLAI V. SOBOLEV,

Institute of Mineralogy and Petrography, Russian Academy of Sciences, Novosibirsk 630090, Russia

AND SERGEI M. BEZBORODOV

ALROSA Co. Ltd., Mirny 678170, Sakha Republic (Yakutia), Russia

Abstract

For the first time, three-dimensional, high-resolution X-ray computed tomography (HRXCT) of an eclogite xenolith from Yakutia has successfully imaged diamonds and their textural relationships with coexisting minerals. Thirty (30) macrodiamonds (≥ 1 mm), with a total weight of just over 3 carats, for an ore grade of some 27,000 ct/ton, were found in a small ($4 \times 5 \times 6$ cm) eclogite, U51/3, from Udachnaya. Based upon 3-D imaging, the diamonds appear to be associated with zones of secondary alteration of clinopyroxene (Cpx) in the xenolith. The presence of diamonds with secondary minerals strongly suggests that the diamonds formed after the eclogite, in conjunction with metasomatic input(s) of carbon-rich fluids. Metasomatic processes are also indicated by the non-systematic variations in Cpx inclusion chemistry in the several diamonds. The inclusions in the diamonds vary considerably in major- and trace-element chemistry within and between diamonds, and do not correspond to the minerals of the host eclogite, whose compositions are extremely homogeneous. Some Cpx inclusions possess +Eu anomalies, probably inherited from their crustal source rocks. The only consistent feature for the Cpx crystals in the inclusions is that they have higher K_2O than the Cpx grains in the host.

The $\delta^{13}C$ compositions are relatively constant at $-5‰$ both within and between diamonds, whereas $\delta^{15}N$ values vary from $-2.8‰$ to $-15.8‰$. Within a diamond, the total N varies considerably from 15 to 285 ppm in one diamond to 103 to 1250 ppm in another. Cathodoluminescent imaging reveals extremely contorted zonations and complex growth histories in the diamonds, indicating large variations in growth environments for each diamond.

This study directly bears on the concept of diamond inclusions as time capsules for investigating the mantle of the Earth. If diamonds and their inclusions can vary so much within this one small xenolith, the significance of their compositions is a serious question that must be addressed in all diamond-inclusion endeavors.

959

Introduction

APART FROM THEIR ECONOMIC value for jewelry and industrial processes, diamonds are scientifically valuable as samplers of mantle processes at pressures greater than 4.0 GPa (i.e., deeper than 120 km). Whereas the pressure-temperature conditions under which diamond will crystallize are well known, much remains to be learned about the origin of the carbon in diamond, why the carbon nucleates and crystallizes into diamond, when this growth process occurs, and how long it takes.

Being nearly pure carbon, diamonds themselves contain relatively limited information about the chemical conditions under which they crystallized. The aggregation state of nitrogen impurities in diamond increases with time and temperature, which provides a way to calculate the length of time a diamond resided in the mantle at a given temperature (Taylor et al., 1990; Mendelssohn and Milledge, 1995), although this temperature is rarely known with any certainty.

To date, the primary source of information on the growth conditions of diamond has been from investigations of their mineral inclusions. The inclusions of interest are typically eclogitic or peridotitic minerals, and can represent pristine samples of the environment present during diamond growth (unless the diamond cracked and chemical exchange occurred along the cracks). Based upon studies of peridotitic diamond inclusions, it has been suggested that peridotitic diamonds possibly grew under subsolidus conditions (Boyd and Finnerty, 1980; Hervig et al., 1980).

Studies of eclogitic diamond inclusions, however, have yielded enigmatic results. The higher equilibration temperatures of eclogitic diamond inclusions compared to peridotitic inclusions, plus the report that multiple inclusions from a single eclogitic diamond follow an igneous fractionation trend from core to rim in the diamond (Bulanova, 1995), suggested that some eclogitic diamonds may form by igneous crystallization. This could possibly be from a sulfide-silicate melt (Bulanova et al., 1998) or a sulfide-immiscible melt (Haggerty, 1986). However, variations in compositions of multiple inclusions in many other eclogitic diamonds are not systematic (Sobolev et al., 1998a; Taylor et al., 1998; Keller et al., 1999) and require disequilibrium conditions that are inconsistent with igneous fractionation. An additional complication is the discovery of compositional differences between many eclogitic diamond inclusions and the same minerals in the host eclogite xenoliths (Sobolev et al., 1983; Ireland et al., 1994; Taylor et al., 1996; Keller et al., 1999). Thus, either the diamonds and the xenolith were not cogenetic, or the xenolith composition has undergone significant post-diamond chemical modification.

In general, studies of diamond inclusions indicate that diamond growth occurs under variable chemical conditions (Griffin et al., 1988; Sobolev et al., 1998; Taylor et al., 1998; Keller et al., 1999). This can be intermittent over long periods of time (Richardson et al., 1984, 1993, 1997; Taylor et al., 1998; Pearson et al., 1999). Inclusion compositions can be diverse within the same diamond (Griffin et al., 1988; Sobolev et al., 1998a; Taylor et al., 1998) and between different diamonds from the same xenolith (Keller et al., 1999). This would seem to conflict with isotopic studies of multiple inclusions from numerous diamonds (Richardson et al., 1984, 1990, 1993, 1997; Richardson, 1986) that have yielded unique, consistent model and even "isochron" ages. This apparent enigma may be explained if diamonds commonly form by metasomatic processes, such that changes in mantle composition during diamond growth, now seen as variable inclusion compositions, occurred over periods of time so short that they are within the analytical error of isotopic dating techniques.

Diamond growth during metasomatic events, from a carbon-rich fluid passing through the mantle, appears to account for the rapidly changing conditions during diamond growth. It may also explain the problem of the source of carbon for the diamond formation (Deines and Harris, 1994, 1995; Stachel and Harris, 1997; Spetsius and Griffin, 1998; Taylor et al., 1998).

Complementary to the data from diamond inclusion studies is another source of information on diamond genesis: *the mantle rocks in which diamonds occur*. Most diamonds are recovered from kimberlite, but this reflects only how the diamonds were transported to the surface. The mantle rocks, in which the diamonds actually grew, peridotites and eclogites, are largely broken up by turbulent fluid flow in the kimberlitic magma, thereby releasing their diamonds. Peridotites are particularly susceptible to this crushing, being composed of easily altered and relatively weak olivine. However, eclogites, although not as numerous as peridotites in most kimberlitic samplings of the mantle, often remain intact, occasionally as diamondiferous xeno-

liths.[1] These xenoliths contain petrologic and geochemical information on the conditions under which the diamonds grew.

The coarse-grained nature (e.g., 3–10 mm) of the minerals in eclogite xenoliths makes it difficult to choose representative samples to study by thin section or by geochemical analysis. Furthermore, determining the 3-D aspects of the texture of a xenolith would require slicing, preparing, and examining a prohibitively large number of thin sections. As part of a comprehensive study of diamond inclusions, diamond growth, and diamondiferous xenoliths, we have conducted high-resolution X-ray studies of the 3-D nature of a diamondiferous eclogite xenolith (U51/3) from the Udachnaya kimberlite, Yakutia. This was followed by extensive chemical and isotopic investigations of the host eclogite, diamond inclusions, and the diamonds themselves. A preliminary report of our initial attempts at such an investigation was presented by Keller et al. (1999) and by Taylor et al. (1999). A major objective in these 3-D studies is to determine if a complete textural characterization of a diamondiferous xenolith could establish any consistent relationships in the xenolith between the diamonds and other minerals, both primary and secondary. This is an independent test of the hypothesis developed from diamond inclusion studies that diamonds grow along metasomatic fronts in the mantle.

Methodology

The diamondiferous eclogite was first examined by X-ray tomography to determine a 3-D model of the sample. The spatial relationships of the minerals, their textures, and associations were thereby documented. This 3-D imaging also permitted precisely locating the diamonds that allowed for carefully planned extraction. Finding and extracting the diamonds using a series of blind, random cuts would have been far more difficult and destructive. A

series of cuts through the xenolith were made in order to least disturb the diamonds, and the diamonds were extracted. Thin sections were prepared of each diamond site, preserving the textural relations. All diamonds were initially examined with a binocular microscope, followed by cutting and polishing several of the diamonds so as to expose their mineral inclusions. Others were mechanically crushed and their inclusions extracted. The diamonds, their inclusions, and the minerals of the eclogite host were all subjected to detailed chemical analysis.

X-ray tomography technique

High-resolution X-ray computed tomography (HRXCT; Carlson and Denison, 1992; Denison et al., 1997; Rowe et al., 1997) permits the study of the entire volume of a xenolith in three dimensions. This is a non-destructive technique that locates the diamonds and other minerals within the xenolith and reveals their textural relationships. Subjecting the entire xenolith to this technique results in a complete 3-D digital model that can be quantitatively analyzed for spatial and textural relationships using spatial analysis techniques (Carlson et al., 1995; Denison and Carlson, 1997).

In the present study, 3-D HRXCT data were acquired in a series of 2-D slices, using a microfocal X-ray source and an image-intensifier detector system to measure the absorption of X-rays along thousands of different coplanar paths through the sample. The plane containing the X-ray paths is divided into a matrix of cells or pixels (512 × 512 in this study); an X-ray attenuation value is derived for each cell in the matrix using standard tomographic techniques (Denison et al., 1997). Thereby, a 2-D HRXCT image is produced that is a map of the values of the linear attenuation coefficients for the input X-ray spectrum in a particular plane through the sample, in which different colors or levels of grey are assigned to different attenuation values. The total attenuation depends upon the X-ray energy, mass density, and effective atomic number, so proper selection of X-ray energies makes it possible to clearly distinguish diamonds from silicate, oxide, and sulfide minerals within the eclogite specimen.

Spatial relationships between diamonds and their surroundings can provide clues to the processes that control diamond crystallization. These relationships can be determined by rotating and viewing the model at different perspectives and ori-

---

[1] In Yakutia, during the processing of the kimberlite, the ore is crushed to ~5–6 cm size, washed, and passed along a conveyor belt. These golf ball–sized rocks are exposed to X-rays, whereby any diamonds exposed at their surface will fluoresce a bright blue. Sensed by a detector, a shot of compressed air moves the rock off the belt into a rubber bag. There are diamonds present in this sample, and it is handled carefully so as to recover the possibly large diamonds. The diamondiferous eclogites that our group has been studying for several years are from these suites of scientifically invaluable samples.

FIG. 1. HRXCT three-dimensional image of the eclogite xenolith U51, created by stacking the 80 two-dimensional images. The appearances of various phases are the same as those in Figure 2.

entations to look for any associations or alignments. Volume visualization software makes it possible to view any aspect of the 3-D model from any perspective. It is possible to render some of the model as transparent and display only one or two mineral phases at a time. Then by rotating the model, it is possible to look for spatial relationships between different crystals of the same mineral or between different minerals. These visualizations are difficult to display here as 2-D figures (Fig. 1), but an animation of the diamonds, garnets, and clinopyroxenes of this U51 eclogite xenolith rotating in space can be viewed at the following address: http://www.ctlab.geo.utexas.edu/imfoframes/imfoani.html.

A complete 3-D model is more representative of the sample than are thin sections. Modal analyses of five thin sections taken from this U51 xenolith ranged from 25 to 40% garnet. The entire xenolith is actually 25.9% garnet by volume, so most of the thin sections are poor representations of the complete xenolith. This results partly from the coarse grain size of the xenolith compared to the size of a thin section. Also, the location of a thin section is com-

monly chosen to include some interesting feature, rather than to accurately represent the entire volume of the rock.

Chemical and isotopic analytical techniques

Major- and minor-element compositions of minerals were determined with a Cameca SX-50 electron microprobe at the University of Tennessee. Minerals and metals were used as standards. Analytical conditions employed an accelerating voltage of 15 keV, a beam current of 20 nA, beam size of 5 μm, and 20 second counting times for all elements, except K in clinopyroxene and Na in garnet (60 seconds each). All analyses underwent a full ZAF correction. Cathodoluminescence (CL) images of diamonds were collected on the EMP by beam rastering and translation of the sample stage. Each frame of the CL images is 384 μm × 384 μm in size.

Concentrations of REE and other trace elements were obtained using a Secondary Ion Mass Spectrometer (SIMS, Cameca IMS 3f) at the Tokyo Institute of Technology. A well-calibrated augite megacryst from an alkali basalt in Japan and a quenched glass of JB-1 rock were used as standards. An energy-filtering technique with an offset voltage of –40V for REE and –100V for other trace elements was applied to eliminate possible molecular interference. The primary ion beam $^{16}O^-$ was about 20 μm in diameter. Analytical uncertainties are 10–20% for REE and 5–10% for other trace elements. Details of the SIMS technique were presented in Yurimoto et al. (1989).

Isotopic compositions of carbon and nitrogen, and the concentrations of nitrogen in micro-areas on the surfaces of polished diamonds were analyzed using the SIMS (Cameca IMS 6f) at the Carnegie Institution of Washington. Carbon isotopes were measured using an Cs^+ ion beam (0.5–2.0 nA) and collection of negatively charged C-ions at low mass resolution and high energy offset (+250 ± 100 eV). Nitrogen isotopes and concentrations were determined using the $^{15}N^{12}C/^{14}N^{12}C$ ratio to measure $\delta^{15}N$ in nitrogen-bearing diamonds, because nitrogen itself does not ionize appreciably by sputtering. The analysis used a Cs^+ ion beam (5–40 nA, depending on N concentration) and collection of negatively charged CN molecules at high mass resolution (MRP = 7000–9000). The analytical uncertainties are ±0.6‰ for $\delta^{13}C$, ±3‰ for $\delta^{15}N$, and ±10 % in nitrogen concentrations. Details about the analytical techniques were presented by Hauri et al. (1999).

3-Dimensional Imaging

The sample employed in this study (U51-3) is a diamond-bearing eclogite xenolith from the Udachnaya kimberlite pipe in Yakutia, with a dimension of ~ 4 × 5 × 6 cm. Several diamonds (11) were exposed on its surface, and the garnet (Gt) and clinopyroxene (Cpx) are coarse grained (i.e., 3–10 mm), and most grains are unweathered. The entire volume of the sample was mapped with a series of 80 HRXCT slices at a slice thickness of 0.5 mm, using a microfocal X-ray source operating at 100 kV and 0.4 mA. This provided optimum contrast between the minerals present with an in-plane resolution of better than 100 microns. Beam-hardening artifacts, caused by preferential absorption of lower energy X-rays, result in darkening of an image towards its center; these were minimized by embedding the sample in powdered garnet and correcting for absorption measured in a scan through the garnet powder alone. Such a 3-D model can also be used to determine the best means for dissection of the xenolith to carefully extract the diamonds, with minimum disturbance of the adjacent minerals.

The diamonds present in U51 were easily distinguished from the other minerals using this high-resolution X-ray tomography technique (Fig. 2). This is in contrast to a previous XCT experiment on a diamondiferous rock (Schulze et al., 1996), which was not able to resolve diamonds from the silicate minerals. That study did locate some diamonds, but only where they were rimmed by a much denser mineral (barite).

Based on these HRXCT digital results, it is possible to determine the mineralogical constitutions of the xenolith with much higher precision than by normal point-counting techniques on thin sections. The eclogite xenolith consists of 25.9 vol% red-orange garnets up to 1 cm in diameter, 0.5% Fe-Ni sulfides up to 3 mm in diameter, and 0.5% macrodiamonds (~1 mm) up to 4 mm in diameter (total weight: 3.0+ carats). All of these diamonds are dispersed in a variably altered matrix of dark green (where unaltered) clinopyroxene that makes up 73.1% of the sample. Diamonds and sulfides are in unusually high proportions in this sample, which makes it an ideal candidate for studying potential genetic relationships between these two minerals.

In total, 30 macrodiamonds (≥1 mm) were found and examined from eclogite U51, and they were labeled alphabetically with letters from A to Z, then AA, etc. Of these 30 diamonds, 18 were wholly
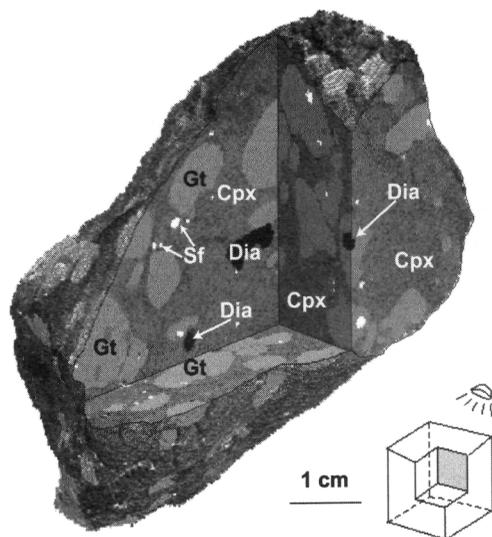
FIG. 2. Two-dimensional HRXCT "slices" (1.5 mm apart) through the U51 diamondiferous eclogite xenolith from Udachnaya. Darkness in this grey-scale image corresponds inversely with a combination of density and effective atomic number factors. The dark grey to black shapes near the center and upper edges of the image are diamonds (Dia). The numerous small white spots are sulfide minerals (Sf), and the light-grey blobs are garnets (Gt), all in a matrix of clinopyroxene (Cpx = medium grey) with a linear (planar in 3-D) alteration fabric (thin, slightly darker grey lines). Although it is not always clear in the HRXCT data, hand-sample and thin-section observations confirm that all of the diamonds in this sample are associated with Cpx alteration.

within or between Cpx, 12 occurred between Gt and Cpx, and none was entirely within Gt. Through a combination of HRXCT and hand sample/thin-section observations, it is evident that the diamonds are always surrounded by secondary minerals, and are nowhere in contact with fresh Gt or Cpx. The sulfide minerals, while similar to the diamonds in total volume, are smaller and more numerous, and occur within and between both Gt and Cpx (Fig. 1). In hand sample, all of the Gts can be seen to have kelyphytic rims, but are otherwise fresh. Garnets that abut diamonds do not appear to be different from those that abut Cpx and vice versa. Also, Cpx occurs as inclusions in Gt and vice versa. The majority of the Cpx is fresh, but is permeated by a fabric of sub-planar cracks. A narrow zone of secondary mineralization occurs along each of these cracks. The lower density (i.e., greater X-ray attenuation) of these

TABLE 1. Major-Element Average Compositions of Minerals in Eclogite Xenolith U51[1]

| | | | U51-3b | |
| Phase: | Clinopyorxene | Garnet | Garnet rim | Garnet core |
No. of analyses:	37	32	15	3
SiO_2	55.3 (3)	40.8 (2)	40.7 (4)	41.0 (1)
Al_2O_3	8.50 (10)	22.6 (1)	22.5 (1)	22.8 (1)
TiO_2	0.47 (4)	0.34 (5)	0.41 (4)	0.28 (3)
Cr_2O_3	0.08 (2)	0.07 (2)	0.09 (2)	0.09 (3)
FeO	5.61 (10)	16.0 (2)	15.7 (1)	15.7 (2)
MnO	0.08 (2)	0.31 (2)	0.32 (3)	0.31 (3)
MgO	11.6 (1)	16.6 (2)	16.1 (2)	16.7 (2)
CaO	12.1 (1)	3.46 (27)	3.85 (19)	3.15 (4)
Na_2O	5.51 (6)	0.14 (2)	0.16 (1)	0.13 (1)
K_2O	0.07 (1)			
Total	99.25	100.45	99.87	100.19
Oxygen basis	6	12	12	12
Si	1.991	2.977	2.986	2.989
Al	0.360	1.946	1.945	1.959
Ti	0.013	0.019	0.023	0.015
Cr	0.002	0.004	0.005	0.005
Fe	0.169	0.977	0.963	0.957
Mn	0.002	0.019	0.020	0.019
Mg	0.620	1.806	1.761	1.815
Ca	0.465	0.271	0.303	0.246
Na	0.384	0.020	0.023	0.018
K	0.003			
Total	4.009	8.039	8.028	8.023
Mg#	78.6	64.9	64.6	65.5

[1]Numbers in parentheses are standard deviations given for the last decimal place cited.

alteration zones render them visible as thin dark lines through the Cpx in the HRXCT data (Fig. 2).

Host Eclogite Mineralogy

Clinopyroxenes in the host eclogite xenolith (U51) are omphacitic, with Na_2O contents of 5.4–5.7 wt% (Table 1). End-member compositions are Wo (37-38), En (49-50), and Fs (13-14). No evident chemical zonations were detected in individual grains, and Cpxs are chemically homogeneous throughout the xenolith. The compositions of Cpxs plot within the field of Group B eclogites in the MgO versus Na_2O plot (Fig. 3C) of Taylor and Neal (1989). In comparison with Cpx in other eclogite

xenoliths from the same Udachnaya kimberlite pipe, most of which are also diamondiferous, those from U51 show moderate MgO, Al_2O_3, and Na_2O contents, but relatively higher contents of TiO_2 (Fig. 3A). Here, it should be emphasized that contents of K_2O in Cpx of the host eclogite U51 are uniformly low (0.07 wt%) (Fig. 3B), even lower than most other eclogite xenoliths from the same kimberlite pipe (Sobolev et al., 1994).

The garnet in the host eclogite is pyropic, with an end-member composition of grossular 9%, pyrope 59%, and almandine 32%. Most Gt grains are chemically homogeneous. However, zonation was detected in some of the largest Gts, which show slightly more Mg-rich cores (60 mol% pyrope; see
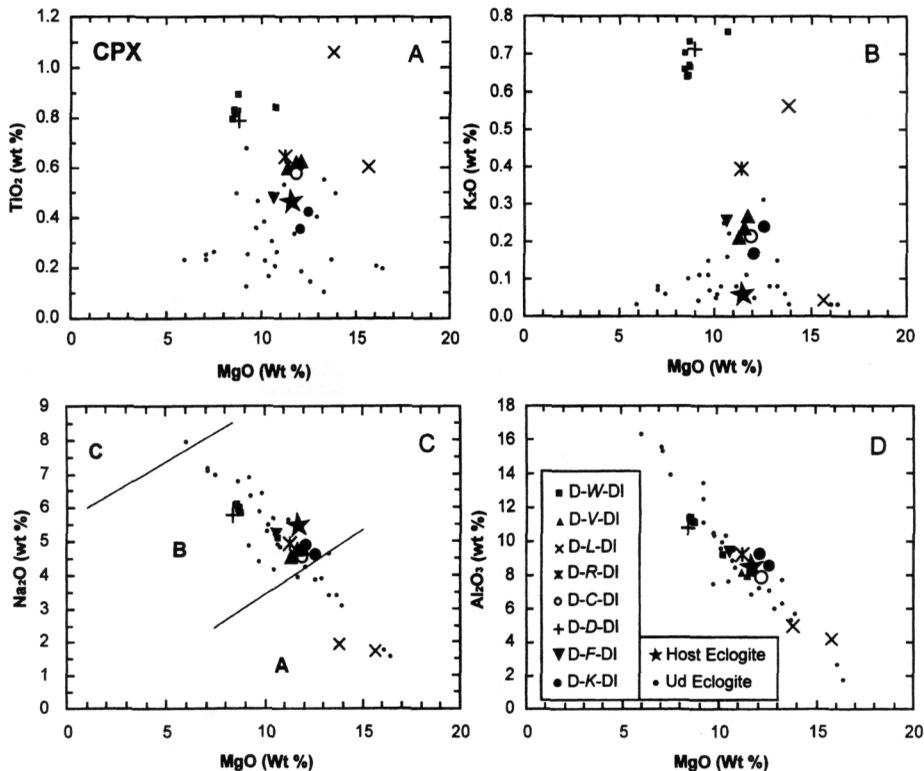
FIG. 3. Primary major-element compositions of Cpx inclusions in diamonds from the eclogite xenolith U51, in comparison with those from the host eclogite and other eclogite xenoliths from the same Udachnaya kimberlite pipe (Sobolev et al., 1994). These Cpx inclusions cover a very wide compositional range, and are different from the host eclogite. The letters A through W represent some of the individual diamonds recovered from this xenolith.

Table 1). In comparison with many other eclogite xenoliths from the same kimberlite pipe, Gts in U51 show moderate contents of TiO$_2$ and MnO, but contain more abundant Na$_2$O and MgO (Fig. 4). Average content of MgO in Gts from U51 is 16.6 wt%; in contrast, MgO contents in Gts of most other eclogite xenoliths from the same kimberlite pipe are less than 15 wt%. As a result, U51 plots at the boundary of Group A and Group B ecolgites, as depicted in Figure 5.

Because of the general homogeneities of the Gts and Cpxs in U51, it is reasonable to consider that chemical equilibrium between Gt and Cpx had been achieved. Pressure and temperature are among the most important parameters to constrain the formation of mantle-derived materials, which can be obtained using the Fe/Mg partitioning between Gt and Cpx, based upon the experimental calibration of Ellis and Green (1979). Application of this Fe/Mg exchange geothermometer requires an independent estimate of pressure, which usually is not directly

available from the mineral chemistry of eclogite alone. In this case, equilibrium pressure and temperature can be estimated by requiring a simultaneous solution with the ambient geothermal gradient of the craton. Studies of mantle xenoliths (Boyd et al., 1997) and xenocrysts (Griffin et al., 1996) from Yakutian kimberlites have demonstrated that the geotherm of the Siberian craton is close to 40 mW/m^2. Using this integrated method of temperature estimation coupled with assumed presence of the eclogite on the geotherm, the estimated temperature is about 1260°C with a pressure of 6.5 GPa (Fig. 6), corresponding to a depth of 180 km in the mantle. These values are well within the stability field of diamond, and consistent with the presence of diamonds in this eclogite xenolith.

Sulfide minerals (pyrrhotite, pentlandite, chalcopyrite) are present in this eclogite, some as inclusions in Gt and Cpx. Re and Os isotopic compositions of these phases were determined, and the
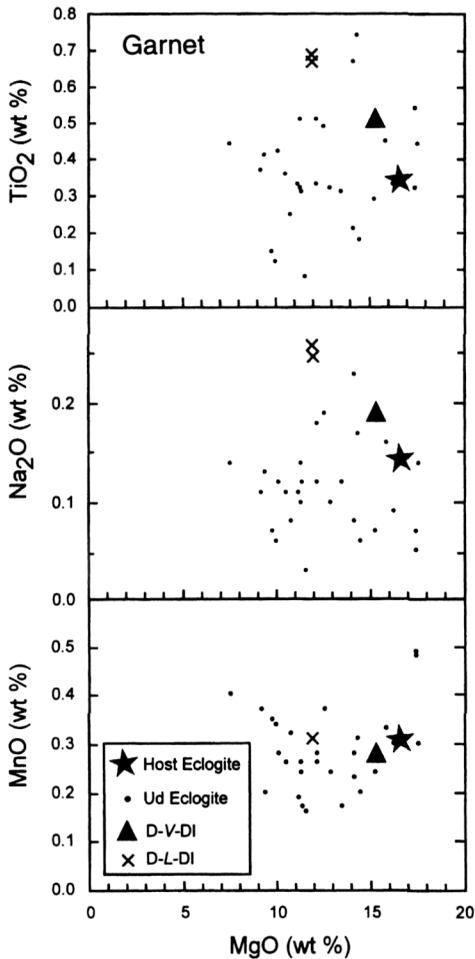
FIG. 4. Major-element compositions of garnet inclusions in diamonds from the eclogite xenolith U51, in comparison with those from the host eclogite and other diamondiferous eclogite xenoliths from the same Udachnaya kimberlite pipe (Sobolev et al., 1994). These inclusions are richer in TiO_2 and Na_2O than Gts in the host eclogite.

FIG. 5. Ca-Mg-Fe plot of Gt inclusions in diamonds, in comparison with those from the host eclogite and other eclogite xenoliths from the same Udachnaya kimberlite pipe (Sobolev et al., 1994).
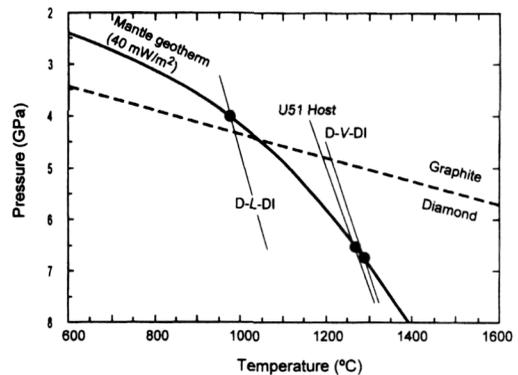
FIG. 6. Estimation of equilibrium pressure and temperature of the host eclogite xenolith and mineral inclusions in diamonds.

results are summarized in Table 2. The ratios of $^{187}Re/^{188}Os$ spread over a large range (from 2.702 to 8.099). This spread yields an isochron age of 2.6 ± 0.6 Ga (Fig. 7) and an initial $^{187}Os/^{188}Os$ of 0.64. Although this age and initial ratio are similar to those for a whole-rock isochron for Udachnaya eclogites (2.90 ± 0.38 Ga and 0.50, respectively) (Pearson et al., 1995), *this is the first known internal Re-Os isochron for an eclogite.*

Oxygen isotopic compositions were determined by the laser-fusion technique, on clean mineral separates of Cpx and Gt from this eclogite (Snyder et al.,

1995). The $\delta^{18}O$ values for the Cpx and whole rock of this eclogite are 7.02‰ and 7.26‰, respectively. It is apparent that these values are well above the accepted mantle values of 5.4‰. This is explained as the result of relatively low temperature hydrothermal alteration of oceanic crust prior to its subduction and underplating of the Siberian craton at almost 3 Ga (Snyder et al., 1997). Such an origin is similar to that for many eclogites from southern Africa (Taylor, 1993).

Mineral Inclusions in Diamonds

As an extraordinary feature of the diamond-bearing eclogite xenolith U51, 8 of the total of 30 dia-

TABLE 2. Re-Os Isotopic Compositions of Sulfide-Silicate Phases from Eclogite U51[1]

	Re, ppb	Os, ppb	$^{187}Re/^{188}Os$	$^{187}Os/^{188}Os$
Garnet-sufide	0.254	0.169	8.099	0.990 (3)
Pyroxene-sulfide	0.346	0.668	2.702	0.7542 (7)

[1]Uncertainties on $^{187}Re/^{188}Os$ and $^{187}Os/^{187}Os$ are estimated at 1%.
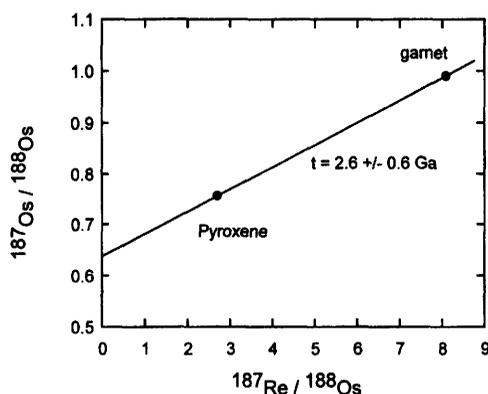
FIG. 7. Re-Os isochron age from sulfide inclusions in Gt and Cpx from the eclogite xenolith U51.

monds contain mineral inclusions. These invaluable diamond inclusions supply important information to constrain the formation of diamonds and the chemical evolution of the host eclogite. In all, 28 inclusions were recovered, among which only 3 are garnets; all others are Cpx. Grain sizes of these diamond inclusions are 20–100 μm. Some diamond inclusions exhibit euhedral crystal shapes, but most Cpxs are irregular in shape, particularly those with extensive secondary alteration. The three Gt inclusions are fresh, and no secondary alterations are observed. Figure 8 shows backscattered electron (BSE) images of two Cpx inclusions from diamond "W." The secondary "spongy" texture can be easily distinguished from the primary Cpx. This texture results from metasomatically induced partial melting of Cpx, where K-rich fluids have attacked the primary Cpx, forming a Na-depleted Cpx plus spinel, with a residual melt present as K-, Na-, and Al-rich glass (Spetsius and Taylor, 2001). It seems probable that a metasomatic fluid penetrated cracks in this diamond to create these partial-melting effects.

Major-element compositions

Diamond inclusions of both Cpx and Gt are significantly different in chemical composition from those in the host eclogite. Major-element compositions of the primary Cpx and Gt inclusions are summarized in Table 3, and plotted in Figures 3–5, where they are also compared to the host eclogite and other diamondiferous eclogite xenoliths from the Udachnaya kimberlite pipe (Sobolev et al., 1994). Despite the fact that all these inclusions are in diamonds from only a single eclogite xenolith, *the major-element compositions of the diamond inclusions vary significantly. Notably, the multiple inclusions from the same diamond are different.* Eight Cpx inclusions from diamond "W" show generally constant major-element compositions, except for DI-W-2, which is relatively richer in MgO (10.7 versus 8.5 wt%). Similar features were also observed from inclusions in diamond "V." However, two Cpx inclusions from diamond "L" exhibit contrasting compositions for almost all elements.

Considering all Cpx diamond inclusions from eclogite U51 as a group, TiO_2 contents are 0.35–1.06 wt% (Fig. 3); most values are much higher than the 0.47 wt% TiO_2 of Cpx in the host eclogite, as well as in other diamondiferous eclogites from Udachnaya. The K_2O contents in these Cpx inclusions vary significantly from 0.17 wt% to 0.73 wt%, with the exception of 0.05 wt% in sample D-L-DI-30. In contrast, the highest K_2O content in Cpx from host eclogite xenoliths from the Udachnaya kimberlite pipe (Fig. 3) is only ~0.3 wt%, a contrast first pointed out by Sobolev et al. (1991). The considerably higher content of K_2O in Cpx diamond inclusions compared to those in the host U51 eclogite is an important feature of this xenolith, but was also reported by Taylor et al. (1996, 1998). These differences can be interpreted as indicating the re-equilibration of the host eclogite Cpxs to lower pressures.

Two Cpx inclusions from diamond "L" have low contents of Na_2O and Al_2O_3, compared with other Cpx diamond inclusions. Except for these two, the
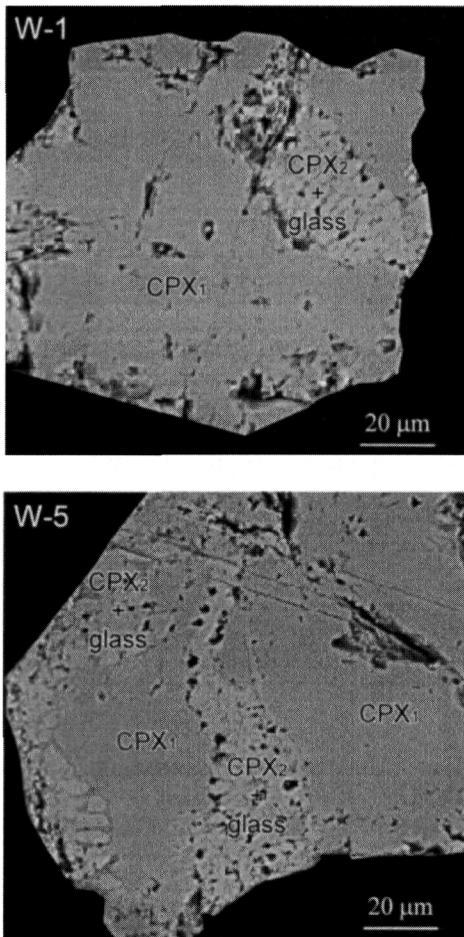
FIG. 8. Omphacitic Cpx inclusions recovered from diamond "W," showing the spongy texture. The spongy part consists of diopside-rich Cpx and interstitial Na, K-rich material formed by partial melting of the primary Cpx, with the participation of metasomatic melt.

other Cpx inclusions show rather limited variations in Na_2O and Al_2O_3 (Figs. 3C and 3D). However, large differences from the host eclogite are still apparent.

Only three Gt diamond inclusions were found in the diamonds. The two Gts from diamond "L" have almost the same major-element compositions, but are considerably different from the Gt inclusion from diamond "V," as shown by considerably higher contents of TiO_2 and Na_2O. In comparison with garnets in the host U51 and other diamondiferous eclogites from Udachnaya, these Gt inclusions contain higher amounts of TiO_2 and Na_2O. However, contents of MgO are distinctly lower than for the Gt in

the host eclogite (Figs. 4 and 5). These compositional features reveal that the Gt and Cpx diamond inclusions are more fertile in these incompatible components than the corresponding minerals in the host eclogite, but in a nonsystematic way.

Assuming that the Cpx and Gt in diamonds "L" and "V" are in equilibrium, P-T estimates can be made. Using the same thermobarometer considerations applied to the host U51 eclogite (Fig. 6), it is estimated that diamond "V" crystallized at 6.7 GPa and 1280°C, in good agreement with that for the host eclogite (6.5 GPa and 1260°C). However, using the same mantle geotherm of 40 mW/m^2, the P-T estimations for diamond "L" are 4.0 GPa and 960°C (Fig. 6), outside the diamond-stability field. These P-T estimations indicate that the crystallization of diamonds in eclogite U51 may have occurred with large variations in pressure and temperature. Alternatively, the Gt and Cpx diamond inclusions could have formed at different times under different chemical and/or P-T conditions.

Trace-element compositions

Trace elements, particularly the rare-earth elements (REEs), in minerals from mantle xenoliths are sensitive to mantle conditions during their formation, and thus may efficiently constrain these processes. In this study, 15 of the larger (>30 μm) diamond inclusions were analyzed for concentrations of REEs and other trace elements. The analytical results are summarized in Table 4.

Eight Cpx inclusions from diamond "W" are similar in REE concentrations with concave-upward patterns. La_n changes from 7.8 to 16.6 and Yb_n from 2.3 to 4.6. As shown in Figure 9A, these inclusions are uniformly enriched in REEs compared to Cpx in the host eclogite, as well as in most other diamondiferous eclogites from Udachnaya (Jerde et al., 1993; Snyder et al., 1997). Similar REE patterns were observed from Cpx inclusions in diamond "L"; however, from grain to grain, their concentrations are significantly different, with La_n of 1.2 to 26.9 and Yb_n from 1.1 to 4.7. *The REE concentrations in three Cpx inclusions from the same diamond cover almost the entire range of REE contents in Cpx from all diamondiferous eclogite xenoliths from Udachnaya.* Also, except for sample L26, the another two L Cpx inclusions are much more abundant in REEs than Cpx in the host eclogite (Fig. 9B).

Additionally, *strong +Eu anomalies were detected in these three diamond inclusions.* Similar REE features were also observed from Cpx inclusions in

Table 3 Major-Element Compositions of the Primary Diamond Inclusions from Eclogite U51

DI:	Clinopyroxene																			Garnet		
	W-1	W-2	W-4	W-5	W-10	W-12	W-14	W-17	V-19	V-21	V-23	R-25	L-29	L-30	Dia C	Dia D	Dia F	Dia K1	Dia K2	V-22	L-27	L-31
No. of analyses:	4	4	4	5	4	1	3	1	3	1	3	3	3	3	5	2	3	7	30	2	3	2
SiO$_2$	55.3	55.2	55.2	55.0	55.0	54.8	55.3	55.1	54.8	53.9	55.2	55.4	52.7	52.7	55.5	54.9	54.5	54.6	55.9	40.7	39.9	40.6
Al$_2$O$_3$	11.2	9.2	11.2	11.2	11.3	11.1	11.4	11.1	8.27	8.34	8.15	8.55	5.01	4.27	8.19	11.19	9.44	8.72	8.67	22.3	21.8	22.3
TiO$_2$	0.81	0.84	0.82	0.82	0.79	0.82	0.83	0.89	0.62	0.61	0.62	0.62	1.06	0.60	0.58	0.80	0.48	0.35	0.42	0.51	0.69	0.67
Cr$_2$O$_3$	0.05	0.06	0.04	0.05	0.10	0.02	0.04	0.11	0.12	0.12	0.10	0.07	0.06	0.08	0.14	0.03	0.12	0.09	0.10	0.09	0.04	0.04
FeO	5.11	5.50	5.09	5.01	4.95	4.91	4.98	4.84	5.56	5.62	5.68	5.71	6.11	5.79	5.55	4.78	5.38	5.61	5.85	15.7	18.2	17.5
MnO	0.06	0.08	0.05	0.05	0.06	0.08	0.06	0.07	0.10	0.06	0.09	0.07	0.07	0.10	0.09	0.06	0.05	0.08	0.10	0.28	0.31	0.31
MgO	8.61	10.7	8.72	8.72	8.47	8.68	8.55	8.76	11.8	11.4	11.7	11.4	13.7	15.6	11.8	8.6	10.5	12	12.5	15.3	11.9	11.9
CaO	11.5	12.1	11.6	11.4	11.3	11.5	11.4	11.4	12.6	12.7	12.8	12.1	18.0	18.1	12.8	11.36	12.1	11.8	11.9	4.81	6.73	6.48
Na$_2$O	5.93	5.08	5.98	5.91	6.04	5.99	6.09	5.83	4.73	4.60	4.72	4.81	1.95	1.75	4.58	5.81	5.21	4.90	4.61	0.19	0.26	0.25
K$_2$O	0.64	0.76	0.67	0.67	0.66	0.64	0.70	0.73	0.27	0.22	0.23	0.40	0.57	0.05	0.22	0.71	0.26	0.17	0.24	0.03	0.03	0.03
Total	99.24	99.52	99.41	98.86	98.7	98.5	99.34	98.8	98.91	97.22	99.32	99.08	99.24	99.01	99.45	98.19	98.08	98.32	100.28	99.84	99.78	100.0
Oxygen basis	6	6	6	6	6	6	6	6	6	6	6	6	6	6	6	6	6	6	6	12	12	12
Si	1.983	1.983	1.978	1.980	1.982	1.979	1.980	1.982	1.982	1.977	1.988	1.995	1.939	1.937	1.993	1.985	1.983	1.981	1.986	2.992	2.990	3.016
Al	0.473	0.390	0.473	0.475	0.480	0.472	0.481	0.471	0.353	0.361	0.346	0.363	0.217	0.185	0.347	0.477	0.405	0.373	0.363	1.932	1.925	1.953
Ti	0.022	0.023	0.022	0.022	0.021	0.022	0.022	0.024	0.017	0.017	0.017	0.017	0.029	0.017	0.016	0.022	0.013	0.010	0.011	0.028	0.039	0.037
Cr	0.001	0.002	0.001	0.001	0.003	0.001	0.001	0.003	0.003	0.003	0.003	0.002	0.002	0.002	0.004	0.001	0.003	0.003	0.003	0.005	0.002	0.002
Fe	0.153	0.165	0.153	0.151	0.149	0.148	0.149	0.146	0.168	0.172	0.171	0.172	0.188	0.178	0.167	0.145	0.164	0.170	0.174	0.965	1.141	1.087
Mn	0.002	0.002	0.002	0.002	0.002	0.002	0.002	0.002	0.003	0.002	0.003	0.002	0.002	0.003	0.003	0.002	0.002	0.002	0.003	0.017	0.020	0.020
Mg	0.460	0.573	0.466	0.468	0.455	0.467	0.456	0.470	0.636	0.623	0.628	0.612	0.752	0.855	0.632	0.464	0.569	0.649	0.662	1.677	1.329	1.318
Ca	0.442	0.466	0.445	0.440	0.436	0.445	0.437	0.439	0.488	0.499	0.494	0.467	0.710	0.713	0.492	0.440	0.472	0.459	0.453	0.379	0.540	0.516
Na	0.412	0.354	0.415	0.412	0.422	0.419	0.423	0.407	0.332	0.327	0.330	0.336	0.139	0.125	0.319	0.407	0.367	0.345	0.318	0.027	0.038	0.036
K	0.029	0.035	0.031	0.031	0.030	0.029	0.032	0.034	0.012	0.010	0.011	0.018	0.027	0.002	0.010	0.033	0.012	0.008	0.011	0.003	0.003	0.003
Total	3.978	3.993	3.986	3.981	3.981	3.987	3.984	3.977	3.995	3.993	3.990	3.983	4.005	4.016	3.981	3.974	3.990	3.998	3.984	8.026	8.027	7.988
Mg#	75.0	77.6	75.3	75.6	75.3	75.9	75.4	76.3	79.1	78.3	78.6	78.1	80.0	82.8	79.1	76.2	77.7	79.2	79.2	63.5	53.8	54.8

TAYLOR ET AL.

TABLE 4. Trace-Element Compositions of Clinopyroxene and Garnet Inclusions in Diamonds from Eclogite U51

ppm	W-1	W-2	W-4	W-5	W-10	W-12	W-14	W-17	L-27	L-29	L-39	R-25	V-19	V-23	C	D2	K1	K2	L-26
La	1.92	1.97	1.94	1.88	1.82	2.35	1.86	3.90	0.29	2.28	6.31	0.52	0.28	0.46	0.94	3.13	0.67	1.09	0.77
Ce	4.43	5.18	4.31	4.41	4.54	5.87	4.42	7.13	0.61	5.02	16.03	2.27	1.21	1.29	1.81	6.83	1.92	3.02	1.87
Pr	0.75	0.97	0.70	0.75	0.91	1.03	0.82	1.04	0.22	0.76	2.32	0.62	0.32	0.27	0.54	1.40	0.34	0.46	0.14
Nd	4.35	6.13	4.52	4.43	4.45	5.43	4.29	6.08	2.33	4.33	9.49	4.38	2.27	2.23	5.73	7.50	2.66	3.23	0.43
Sm	2.09	2.48	1.96	1.92	2.10	2.23	1.95	2.93	2.82	1.69	2.36	2.56	1.95	1.57	2.83	2.33	1.01	1.39	0.13
Eu	0.81	1.05	0.79	0.76	0.96	0.87	0.79	1.97	1.63	5.66	1.42	0.87	0.81	0.75	1.30	1.26	0.51	0.86	0.27
Gd	1.96	2.95	1.91	1.90	1.88	2.04	1.83	2.24	4.85	1.61	2.90	2.66	2.02	1.80	2.89	2.79	1.11	1.53	0.12
Tb	0.27	0.41	0.28	0.27	0.29	0.32	0.27	0.38	0.97	0.22	0.43	0.34	0.32	0.30	0.68	0.45	0.20	0.33	0.02
Dy	1.16	1.97	1.32	1.14	1.16	1.37	1.27	1.73	9.24	1.13	1.33	2.00	1.66	1.77	3.88	3.34	1.39	1.47	0.16
Ho	0.23	0.34	0.20	0.21	0.23	0.19	0.18	0.32	1.94	0.26	0.24	0.29	0.28	0.30	0.70	0.72	0.27	0.32	0.03
Er	0.55	0.78	0.43	0.53	0.64	0.47	0.51	0.63	6.98	0.68	0.78	0.88	0.61	0.90	2.01	1.95	0.55	0.78	0.13
Tm	0.08	0.14	0.09	0.08	0.09	0.06	0.06	0.12	1.09	0.07	0.13	0.12	0.11	0.10	0.45	0.45	0.04	0.13	0.03
Yb	0.48	0.75	0.55	0.50	0.56	0.37	0.42	0.42	6.74	0.35	0.77	0.72	0.72	0.85	1.96	1.87	0.47	0.39	0.17
Lu	0.08	0.06	0.06	0.06	0.08	0.06	0.07	0.10	1.14	0.06	0.08	0.11	0.12	0.12	0.49	0.28	0.03	0.05	0.02
Sc	14.0	16.9	16.3	13.1	15.1	23.4	12.8		54.5	14.2	9.8	16.2	15.2	15.9	20.0	23.9	19.2	17.7	
Ti	4835	4666	5088	4609	5061	6485	4635		4273	5598	3326	4087	3687	3654	3605	5450	2058	2584	
V	332	304	379	341	360	458	330		131	369	237	320	283	289	255	470	206	237	
Cr	348	376	427	377	492	502	484		381	443	302	609	970	840	1134	641	850	962	
Sr	266	271	270	252	303	372	248		11.5	234	223	317	295	251	243	184	96	181	
Zr	32.5	21.1	27.6	27.9	41.8	44.4	31.8		59.2	30.6	30.1	11.2	10.2	9.0	7.5	30.5	5.6	7.2	
Hf	1.39	1.45	1.69	1.23	2.46	4.81	1.10		1.76	1.57	2.09	0.99	0.57	1.34	1.70	1.50	0.50	0.80	
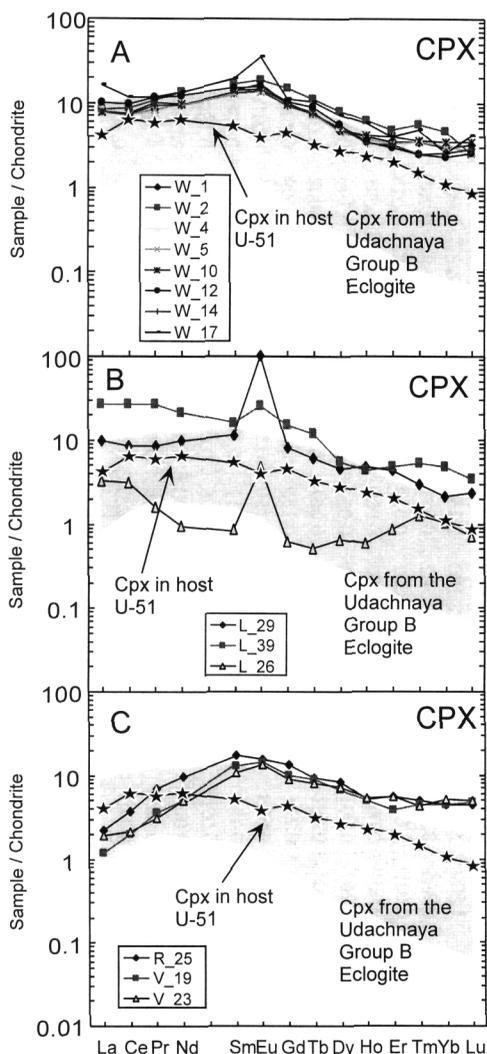
FIG. 9. Chondrite-normalized REE patterns of Cpx and Gt inclusions. Counterparts from the host eclogite and other eclogite xenoliths from the same Udachnaya kimberlite pipe are shown for comparison.

FIG. 10. Chondrite normalized REE pattern of Gt inclusion from diamond "L," which contains more abundant REEs than Gt in the host eclogite.

Only one Gt inclusion from the diamond "L" was large enough for trace-element analysis. The REE pattern is generally parallel to that for the Gt in the host eclogite, but greatly enriched overall (Fig. 10). For example, La_n in the Gt inclusion is about 1.24, much higher than 0.05 in the host Gt. Yb_n in the Gt is 41.5 versus 19.7 in the host Gt. This observation is consistent with the differences in major-element variations, as shown in Figure 4.

Secondary partial melting

Some of the Cpx inclusions in diamonds from U51 have experienced secondary partial melting, leading to the formation of "spongy" textured rims (Fig. 8). This alteration occurred due to the presence of numerous cracks in some of the diamonds. The intensity of this secondary alteration varied significantly from grain to grain. For example, sample D-DI-W2 is basically composed of primary Cpx; however, in sample D-DI-L29, alternation spread over the entire crystal, leaving only small "islands" of primary Cpx.

This secondary spongy texture consists of diopside-rich, Na-depleted Cpx, fine-grained crystals (2–4 μm) of spinel, and interstitial glass rich in K, Na, and Al. This was formed by the metasomatic partial melting of the primary omphacitic Cpx, and by the infiltration of melt/fluid through cracks in the host diamonds, probably associated with kimberlitic fluid (Spetsius and Taylor, 2001).

Major-element compositions of the secondary Cpx and interstitial material obtained from three inclusions are summarized in Table 5, and the compositional variations are depicted in Figure 11. The

diamonds "R" and "V" (Fig. 9C). For the three inclusions in diamond "R" and "V," La_n varies from 1.2 to 2.2 and Yb_n from 4.4 to 5.2. However, an extraordinary feature is that they are poorer in LREE contents but richer in MREE and HREE abundances, compared with Cpx in the host eclogite. As documented above for the major-elements, *concentrations of REEs in the Cpx diamond inclusions from this single eclogite xenolith vary significantly between diamonds, as well as among multiple inclusions in a single diamond.*

TAYLOR ET AL.

TABLE 5. Major-Element Compositions of Secondary Phases in Clinopyroxene Inclusions

DI:	D-DI-W1						D-DI-W5								D-DI-W14				
Phase[1]	W1-1 P.cpx	W1-7 P.cpx	W1-2 S.cpx	W1-6 S.cpx	W1-4 glass	W1-5 glass	W5-1 P.cpx	W5-2 S.cpx	W5-7 S.cpx	W5-3 S.cpx	W5-4 glass	W5-5 glass	W5-6 glass	W5-8 glass	W14-1 P.cpx	W14-2 S.cpx	W14-3 S.cpx	W14-4 glass	W14-5 glass
SiO_2	55.1	54.9	52.3	51.4	51.0	52.7	55.1	51.2	52.3	51.8	60.7	59.8	60.1	55.4	55.5	52.3	52.3	59.5	61.2
Al_2O_3	11.2	11.2	3.57	5.15	16.9	10.6	11.3	6.54	6.37	6.40	15.2	18.9	16.39	9.92	11.5	6.64	6.00	17.6	22.5
TiO_2	0.80	0.76	0.81	1.07	0.82	0.90	0.85	1.12	0.82	1.07	0.37	0.28	0.37	0.9	0.79	1.01	0.82	0.71	0.60
Cr_2O_3	0.02	0.00	0.08	0.12	0.00	0.00	0.10	0.13	0.10	0.08	0.00	0.00	0.00	0.07	0.10	0.04	0.04	0.00	0.00
FeO	5.10	5.21	6.60	6.78	3.66	4.74	5.02	6.69	6.54	7.00	1.98	1.16	1.87	5.16	5.13	6.58	6.34	2.95	1.57
MnO	0.10	0.01	0.12	0.12	0.02	0.14	0.04	0.09	0.04	0.08	0.00	0.02	0.03	0.07	0.07	0.09	0.06	0.02	0.05
MgO	8.60	8.70	14.7	13.8	8.05	12.8	8.54	13.0	13.0	13.2	4.03	2.82	2.91	9.92	8.44	12.5	12.5	3.69	0.53
CaO	11.6	11.6	19.6	18.7	9.62	13.2	11.6	17.9	17.2	17.9	6.31	4.23	3.92	15.1	11.4	16.8	16.2	5.57	0.32
Na_2O	5.89	5.81	1.30	1.66	1.30	1.84	5.72	1.95	2.16	1.93	3.80	4.63	3.06	2.02	5.90	2.65	1.90	3.67	4.28
K_2O	0.62	0.68	0.03	0.14	4.36	3.05	0.63	0.04	0.55	0.05	5.94	5.09	8.70	1.65	0.68	0.14	0.49	3.39	4.96
Total	99.03	98.87	99.11	98.94	95.73	99.97	98.9	98.66	99.08	99.51	98.33	96.93	97.35	100.2	99.51	98.75	96.65	97.1	96.01
Oxygen basis										6									
Si	1.980	1.978	1.937	1.907	1.883	1.899	1.981	1.897	1.926	1.903	2.133	2.100	2.142	1.977	1.983	1.928	1.961	2.089	2.124
Al	0.474	0.475	0.156	0.225	0.735	0.450	0.479	0.286	0.276	0.277	0.630	0.782	0.688	0.417	0.484	0.288	0.265	0.728	0.920
Ti	0.022	0.021	0.023	0.030	0.023	0.024	0.023	0.031	0.023	0.030	0.010	0.007	0.010	0.024	0.021	0.028	0.023	0.019	0.016
Cr	0.001	0.000	0.002	0.004	0.000	0.000	0.003	0.004	0.003	0.002	0.000	0.000	0.000	0.002	0.003	0.001	0.001	0.000	0.000
Fe	0.153	0.157	0.204	0.210	0.113	0.143	0.151	0.207	0.201	0.215	0.058	0.034	0.056	0.154	0.153	0.203	0.199	0.087	0.046
Mn	0.003	0.000	0.004	0.004	0.001	0.004	0.001	0.003	0.001	0.002	0.000	0.001	0.001	0.002	0.002	0.003	0.002	0.001	0.001
Mg	0.461	0.467	0.811	0.763	0.443	0.688	0.458	0.718	0.714	0.723	0.211	0.148	0.155	0.528	0.450	0.687	0.699	0.193	0.027
Ca	0.447	0.448	0.778	0.743	0.380	0.510	0.447	0.711	0.678	0.705	0.238	0.159	0.150	0.577	0.436	0.663	0.651	0.210	0.012
Na	0.410	0.406	0.093	0.119	0.093	0.129	0.399	0.140	0.154	0.137	0.259	0.315	0.211	0.140	0.409	0.189	0.138	0.250	0.288
K	0.028	0.031	0.001	0.007	0.205	0.140	0.029	0.002	0.026	0.002	0.266	0.228	0.396	0.075	0.031	0.007	0.023	0.152	0.220
Total	3.980	3.983	4.009	4.012	3.876	3.986	3.969	3.998	4.002	3.997	3.805	3.774	3.808	3.897	3.972	3.997	3.963	3.728	3.654
Ca'^2	0.421	0.418	0.434	0.433	0.406	0.380	0.423	0.434	0.426	0.429	0.469	0.467	0.416	0.459	0.420	0.427	0.420	0.428	0.140
Mg'^2	0.434	0.436	0.452	0.445	0.473	0.513	0.434	0.439	0.448	0.440	0.417	0.433	0.429	0.419	0.433	0.442	0.451	0.395	0.323
Fe'^2	0.145	0.146	0.114	0.123	0.121	0.107	0.143	0.127	0.126	0.131	0.115	0.100	0.155	0.122	0.147	0.131	0.128	0.177	0.537

[1] Pcpx = primary clinopyroxene; S. cpx = secondary clinopyroxene formed by the partial melting; glass = glasses formed by partial melting.

[2] $Ca' = Ca/(Ca+Mg+Fe)$; $Mg' = Mg/(Ca+Mg+Fe)$; $Fe' = Fe/(Ca+Mg+Fe)$.
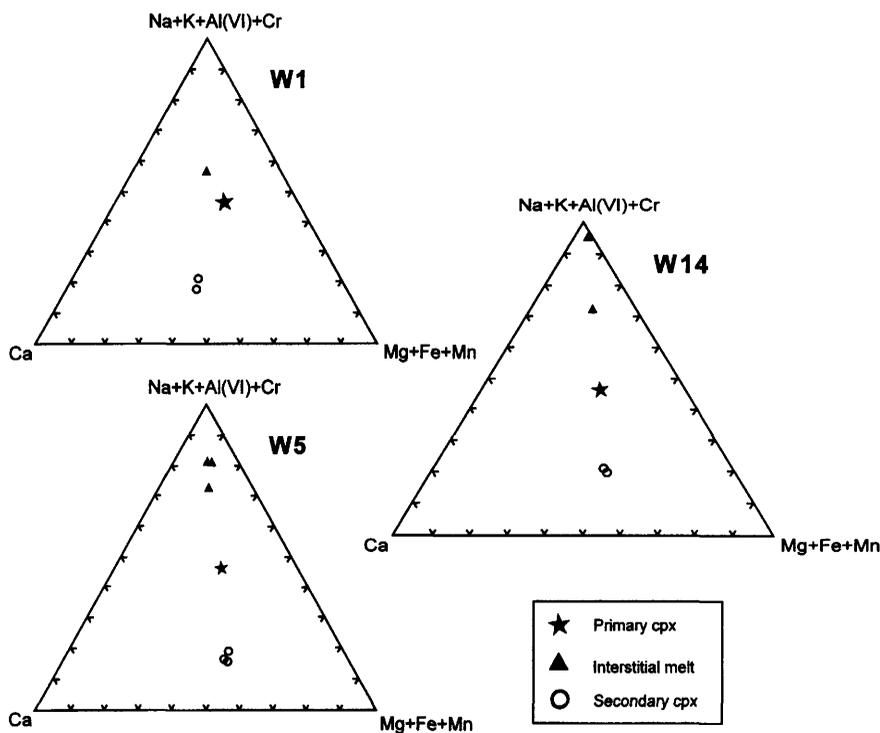
FIG. 11. Major-element compositional variations of the primary Cpx, secondary Cpx, and interstitial materials.

spongy secondary pyroxenes are almost identical to primary Cpx in terms of Ca-Mg-Fe components but are distinctly more diopsidic than the primary Cpx. For example, in D-DI-W1, ratios of Ca:Mg:Fe for both primary and secondary Cpx are around 42:45:13. However, the diopside component $(CaMgSi_2O_6)$ in the primary Cpx is ~ 45%, but in the secondary Cpx it reaches as high as ~ 76%. The secondary Cpxs are consequently poorer in Na_2O, K_2O, and Al_2O_3 (Table 5). Interstitial glasses between the secondary Cpxs are considerably higher in K_2O (up to 8.7%) and Al_2O_3 (up to 18.9%) compared to the primary Cpx. According to Spetsius and Taylor (2001), the overall partial melting reaction can be written as:

$$Cpx_{Primary} + \text{K-rich fluid} = Cpx_{Secondary} +$$

$$\text{spinel} + \text{K-Na-Al-rich glass.}$$
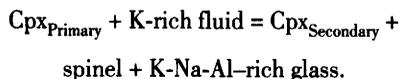
Contrasting behavior of Na_2O reflects the partial melting. Contents of Na_2O in secondary Cpx and interstitial glasses are lower than those in the primary Cpx. In sample D-DI-W1, the Na_2O content in primary Cpx is ~5.9 wt% and decreases to 1–2 wt% in both of the secondary phases. Similar variations also were observed from other samples, as summarized in Table 5. In addition, some chemical heterogeneity was also observed in both the secondary Cpxs and the interstitial materials, particularly in Al_2O_3 and K_2O (Table 5). Except for the decreased Na_2O contents, other chemical features of these phases are comparable with those reported by Taylor and Neal (1989), Fung and Haggerty (1995), and Spetsius and Taylor (2001).

The association of diamonds with secondary minerals is apparently typical of xenoliths from Udachnaya (Spetsius, 1995). This association suggests a metasomatic origin for the diamonds and the secondary minerals, perhaps as a consequence of C-rich fluids passing through the mantle (Deines and Harris, 1994, 1995; Stachel and Harris, 1997; Spetsius and Griffin, 1998; Taylor et al., 1998).

Diamonds

An ideal diamond consists of a lattice of carbon atoms with a Fm3m geometric arrangement. How-
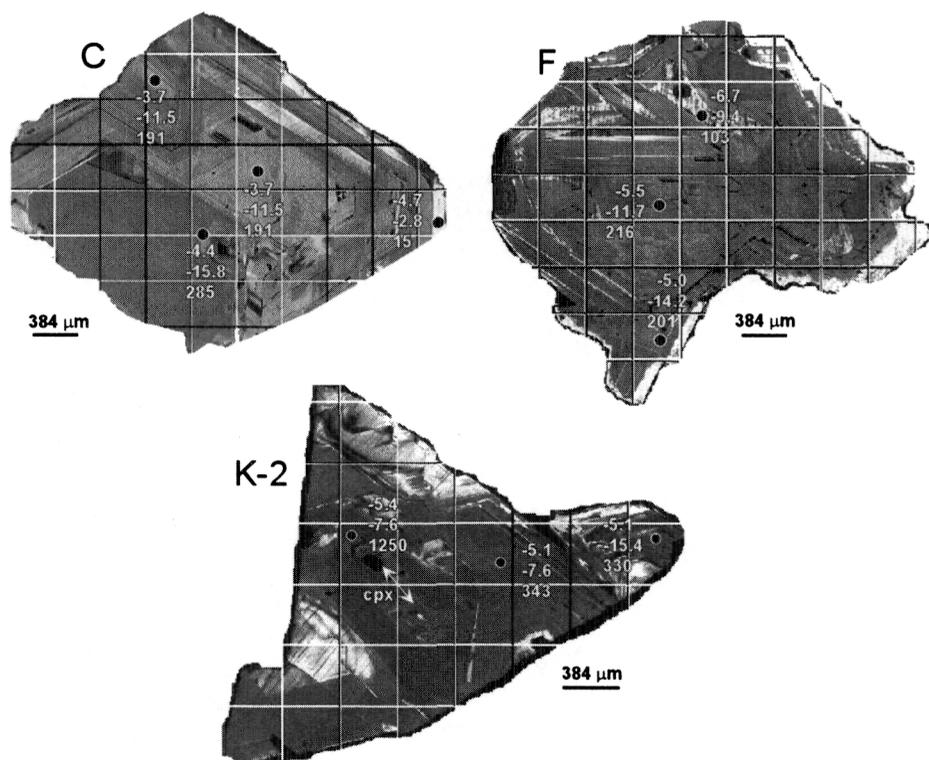
FIG. 12. Cathodoluminescence (CL) images of U51 diamonds. The solid spots show locations of SIMS analysis, with the $\delta^{13}C$ and $\delta^{15}N$ in ‰ and N_{Total} concentration in ppm listed vertically for each spot analyzed.

ever, natural diamonds typically exhibit a considerable number of dislocations and defects, which may act as optical centers for luminescence. The most important one is the substitution of carbon by nitrogen. Other defects include substitution of boron and hydrogen, plastic deformation, and irradiation. All these defects may contribute to the luminescence of diamonds. Cathodoluminescence (CL) is an important technique because differences in luminescence indicate differences in the concentrations of defects and impurities. Thus, CL is an efficient method in investigating the growth history of diamonds (Mendelssohn and Milledge, 1995).

Cathodoluminescence

As revealed by CL examination, a common feature of the diamonds in eclogite U51 is that they have experienced complex episodic growth histories, with initial nucleation and growth followed by resorption and regrowth, accompanied by plastic deformation. It would appear that there was a pro-

gressive chemical/isotopic evolution of the fluid from which the diamond grew, as will be addressed below. In all, 30 diamonds were recovered from the U51 xenolith, among which several crystals (e.g., C, F, K1, K2) were of sufficient size (4 mm) and were cut and polished to expose their inclusions. Samples K1 and K2 are two separate cuts from diamond "K," and another two are diamonds "C" and "F." CL images of these diamonds are shown in Figures 12 and 13.

As illustrated in the CL bands of Figures 12 and 13, large differences in intensities of the CL are evident, and reflect extensive variations of the physical and chemical environment during crystallization of these diamonds (Mendelssohn and Milledge, 1995). These differences are mainly a function of the nitrogen as a common lattice impurity in diamonds. This nitrogen occurs in a variety of "aggregation states," wherein the nitrogen may be present in a simple 1:1 substitution for carbon (Type Ib). At mantle temperatures and pressures, this array of nitrogen is unstable, and the nitrogen
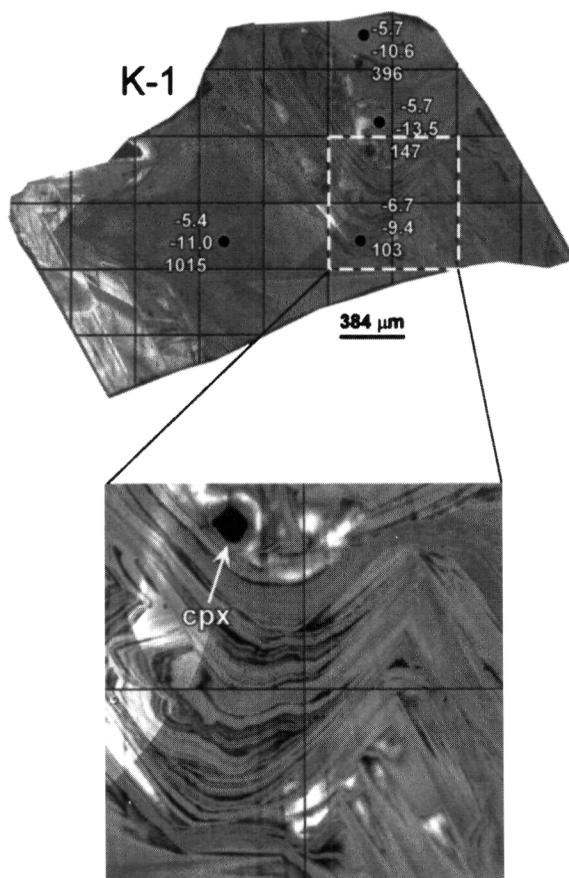
FIG. 13. Magnified CL image of diamond K-1, displaying many narrow growth bands that are extensively folded. The solid spots show locations of SIMS analyses, with $\delta^{13}C$ and $\delta^{15}N$ in ‰ and N_{Total} nitrogen concentration in ppm listed vertically for each spot analyzed.

atoms aggregate rapidly to form pairs (Type IaA). With additional annealing, the pairs actually join together forming groups of four nitrogens (Type IaB).

It is readily apparent that the CL features vary extensively between the individual diamonds, as well as within each. In diamond "C," growth bands are continuous with straight boundaries; however, some complicated zonation can be readily identified in diamond "F," possibly because of episodic growth in which octahedral and cubic growth planes compete for dominance. The enlarged CL image of diamond K1, shown in Figure 13, illustrates the extremely complicated growth that this diamond has undergone, as evidenced by the numerous very fine growth bands. Note the intense folding and deformation of these zones.

Chemistry

Nitrogen concentrations and isotopic compositions of carbon and nitrogen are the most important chemical features of these diamonds. Despite the location of these diamonds in a restricted location within a single xenolith, significant isotopic differences exist both between and within the individual diamonds. The SIMS-analyzed spots and results are labeled on Figures 12 and 13. Concentrations of nitrogen change significantly with position within the zones of the diamonds. For example, in diamond "C," its N concentration is 15 ppm in one region, but in another, it can be as high as 191–285 ppm. Diamond "K" shows the highest nitrogen concentrations, with a range of 103 to 1250 ppm. Comparison of nitrogen concentrations in diamonds from other locales is shown in Figure 14. Most of the analyzed
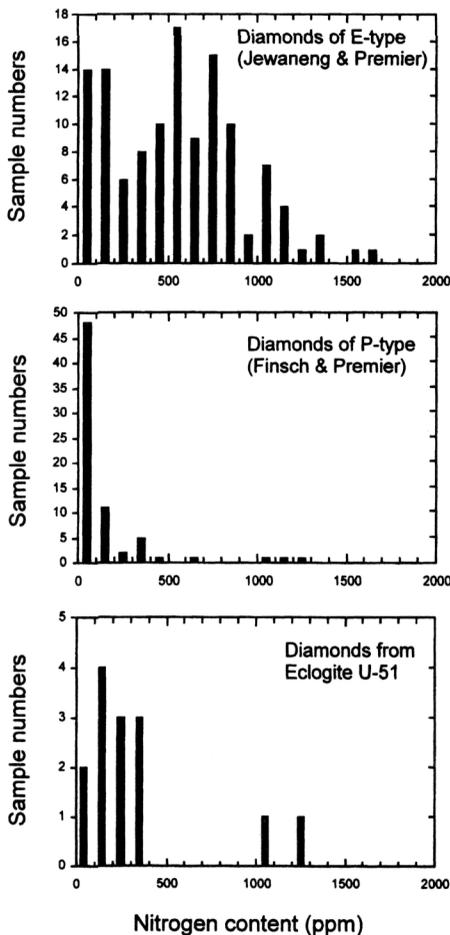
FIG. 14. Nitrogen concentrations in the studied diamonds, in comparison with those from eclogitic diamonds and peridotitic diamonds of worldwide occurrences.

spots contain less than 400 ppm N, but they confirm the observation that nitrogen concentrations are statistically higher in eclogitic diamonds than in peridotitic ones (e.g., Cartigny et al., 1998).

Variations of carbon isotopic compositions are rather limited among these diamonds, but the differences among them are evident. In diamond "C," $\delta^{13}C$ has a range of $-3.7‰$ to $-4.7‰$, $-5.0‰$ to $-6.7‰$ in diamond "F," and $-5.1‰$ to $-6.7‰$ in diamond "K." In contrast, nitrogen shows much larger variations in isotopic compositions than carbon. Diamond "C" has a $\delta^{15}N$ range of $-2.8‰$ to $-15.8‰$, $-9.4‰$ to $-14.2‰$ in diamond "F," and $-7.6‰$ to $-15.4‰$ in diamond "K." However, all but two of the analyzed points have $\delta^{15}N$ between $-7‰$

and $-14‰$. No systematic variations were observed from rim to core in the growth sequences of the diamonds in C, N, or N_{Total}. Correlation between $\delta^{13}C$ and $\delta^{15}N$ for all analyses is shown in Figure 15, in comparison with diamonds from the Jwaneng pipe in Botswana and the No. 50 pipe in China (Cartigny et al., 1998). The most striking feature is that the U51 diamonds have a very narrow range in $\delta^{13}C$, with a peak around $-5‰$. In contrast, $\delta^{15}N$ ratios show a much wider range. The Jwaneng diamonds plotted in Figure 15 are of eclogitic paragenesis. In contrast to the eclogitic diamonds of the present study, the Jwaneng diamonds exhibit a more limited range of $\delta^{15}N$ (0‰ to $-10‰$), but a much wider range of $\delta^{13}C$ ($-5‰$ to $-22‰$). Peridotitic diamonds from the No. 50 kimberlite pipe in China have a similarly wide range of $\delta^{15}N$ and limited range of $\delta^{13}C$ (Cartigny et al., 1998) compared to the studied eclogitic diamonds of U51.

Discussion

Since the pioneering studies of Meyer (1968), Meyer and Boyd (1968), and Sobolev et al. (1972), mineral inclusions in diamonds have been studied extensively, particularly with advances in microbeam techniques. Diamond inclusions are of two parageneses: ultramafic and eclogitic. As defined by their inclusions, diamonds are termed P-type (ultramafic, peridotitic) or E-type (eclogitic). Considering their relations with host diamonds, diamond inclusions in general can be divided into three types: (1) inclusions that crystallized at the same time as the host diamonds are referred to as *syngenetic*; (2) inclusions that are older, being incorporated completely into the growing diamonds, are termed *protogenetic*; and (3) inclusions that resulted from metasomatic infiltration of fluid entering the diamond at some time after crystallization of diamond are described as *epigenetic*. The majority of investigators of diamonds consider the diamond inclusions to be syngenetic; in reality, there are no positive proofs for this gross assumption. In fact, recent studies (e.g., Taylor et al., 1998; Sobolev et al., 1998a; Keller et al., 1999) indicate that many inclusions are obviously older than their encapsulating diamonds (i.e., protogenetic diamond inclusions).

Epigenetic inclusions are usually distinguished from the other inclusion types by cracks in the diamonds connecting the inclusion with the surface of the diamond. These are particularly apparent using CL on an EMP or SEM, where the cracks can be
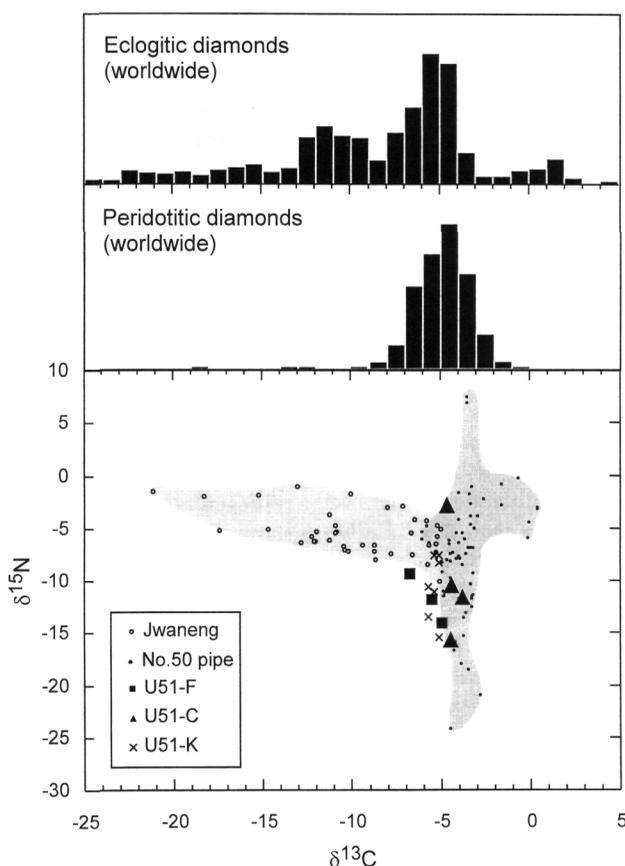
FIG. 15. Correlation of $\delta^{13}C$ and $\delta^{15}N$ of the studied diamonds. Diamonds from the Jwaneng kimberlite in Botswana (eclogitic paragenesis; Cartigny et al., 1997) and those from the No. 50 kimberlite pipe in China (peridotitic paragenesis; Cartigny et al., 1998) are shown for comparison.

readily identified and searched by EDS analysis for the presence of non-diamond components. [This technique was taught to the senior author by Dr. H. Judith Milledge, University College, London.] However, to tell the difference between syngenetic and protogenetic inclusions is more difficult, despite the fact that inclusions in diamonds commonly exhibit an octahedral habit imposed upon the inclusions by the diamond, with its strong "power of crystallization." As a general rule, inclusions of these two parageneses can exist in different diamonds from the same kimberlite pipe; but individual members of one suite do not normally coexist in a single diamond with members of another suite.

Multiple inclusions of one phase in a single diamond can be chemically identical (Meyer, 1987), a relationship that has been utilized to argue that dia-

monds generally formed in a stable P-T-X environment. However, many exceptions to this have been reported. For example, some significant chemical variations among garnets from single diamonds were discovered in a study of eclogitic diamond inclusions from the west Australian diamonds (Griffin et al., 1988). Notable extreme variations were reported by Sobolev et al. (1998a), who observed *large chemical diversities among 35 garnet and 5 Cpx inclusions in a single diamond* from the Mir pipe in Yakutia. Actually, the major- and trace-element compositions of inclusions within this single diamond ranged over almost the entire compositional range of mantle eclogite Cpxs from Yakutia (Sobolev et al., 1998a). Furthermore, in some rare instances, both peridotitic and eclogitic inclusions have been found in single diamond hosts (Prinz et al., 1975;

Hall and Smith, 1985; Otter and Gurney, 1989; Moore and Gurney, 1989; Wang, 1998).

Chemical diversity of diamond inclusions

All inclusions from diamonds in the U51 xenolith are of eclogitic heritage; no inclusions of ultramafic paragenesis were observed. However, these diamond inclusions exhibited very complex compositional features. Four diamonds (K, L, V, W) out of the 30 from this xenolith contain multiple inclusions. Significant compositional variations were observed between Cpx inclusions in the "L" and "W" diamonds. For instance, contents of K_2O vary from 0.05 to 0.57 wt% and 0.64 to 0.76 wt%, respectively (Fig. 3, Table 3). Almost all of the Cpx inclusions are richer in K_2O than the Cpx in the host eclogite, a function of re-equilibration of the host Cpx to lower pressures (Sobolev et al., 1972; Harlow and Veblen, 1991; Taylor et al., 1998; Sobolev et al., 1998b). Large variations in REE concentrations also occur in the Cpxs in diamond "L," including *the presence of +Eu anomalies in the Cpx diamond inclusions*, similar to those reported by Wang (1998). In contrast, Cpxs in diamonds "V" and "K" are homogeneous, in both major and REEs, and without Eu anomalies (Figs. 3and 10C).

A comparison of data for inclusions in the entire population of diamonds in eclogite U51 reveals that the Cpxs exhibit an exceptionally large range of both major- and trace-element contents (Fig. 3). For example, MgO ranges from 8.47 wt% to 15.6 wt%, Na_2O from 1.75 wt% to 6.04 wt%, TiO_2 from 0.35 wt% to 1.06 wt%, and K_2O from 0.05 wt% to 0.76 wt%. As summarized in Tables 1 and 3, Cpx inclusions in diamonds "W," "R," "D," and "F" have Mg# of 75.0–78.3, lower than that of the host Cpx, 78.6. This ratio is much higher in inclusions from other diamonds (79.1–82.8). The three garnet inclusions show consistently lower Mg# (53.8–63.5), compared with 64.9 in the host garnet. Even concentrations of REEs in Cpx inclusions in diamonds "W" and "L" are distinctly higher than that in the host Cpx (Figs. 9A and 9B). However, LREEs in Cpx inclusions in diamonds "R" and "V" are lower than that of the host (Fig. 9C).

The elements K and Na typically exhibit similar geochemical behavior in many circumstances. In partial melting and metasomatic processes, such as may have affected this xenolith, both are typically incompatible elements in mantle silicate systems. However, no consistent variations between these two elements are detected in Cpx inclusions. As shown in Figure 3, some Cpx diamond inclusions contain higher abundances of Na_2O than the host Cpx does, whereas others are lower.

The present study has shown that inclusions in diamonds from a single eclogite xenolith can have a complex variety of chemistries such that it is not obvious how they relate to the conditions of the actual diamond formation. As displayed in Figure 3, *the chemistry of the Cpx diamond inclusions from this one eclogite xenolith covers more than two-thirds of the compositional range of all eclogite Cpxs in xenoliths from the entire Udachnaya kimberlite pipe.*

Chemical diversity of the host ecologite

If it is assumed that the diamond inclusions are representative of the host eclogite at different stages, the range of change in the chemistry of U51 was tremendous, an unlikely situation. In any case, the large variations in chemistry of the diamond inclusions cannot be easily explained as the result of simple partial melting and/or metasomatism of the host eclogite. Instead, the amount and degree of metasomatism must have been abnormally great. We suggest a scenario whereby a CO_2-rich melt/fluid metasomatically invaded an eclogite lithology, and at suitable P-T conditions and oxygen fugacity, crystallization of diamond was initiated. Partial melting of the eclogite may have occurred at this same time, because infiltration of the fluid/melt could lead to a substantial decrease in the solidus temperature.

With changes in P-T and oxygen-fugacity conditions, the chemical composition of the solidus phases could vary greatly, particularly if one also allows for the occurrence of local disequilibrium. The diamonds may halt in their growth, be partially resorbed, and continue additional growth later, all due to these changes in P-T-X conditions. This may lead to the formation of diamonds as observed in Figures 12 and Fig. 13. As a result, minerals captured by growing diamonds at various stages of these processes would exhibit large compositional variations. Garnet and Cpx inclusions in diamond "L" could be incorporated in two different stages in the crystallization history of this diamond.

This scenario, where the inclusions are captured at different periods of the continuing process of chemical change, may explain why they are not truly representative of the host eclogite at all. Indeed, diamond inclusions may be "snapshots" of the eclogite during its evolution. Subsequent recrystallization of the eclogite after formation of the diamonds

could entirely erase any chemical heterogeneities in the host eclogite. However, the large chemical diversity of the inclusions would be perfectly retained, because of encapsulation in the host diamonds.

Chemistry of the diamonds

Stable isotopes in diamonds can provide constraints on the formation of diamond in the mantle. A survey of carbon isotopic data on worldwide occurrences of diamond demonstrate that eclogitic diamonds have a wide range of values, with $\delta^{13}C$ varying from +3‰ to –30‰ (e.g., Deines et al., 1993). In contrast, peridotitic diamonds have a rather limited variation, with most of $\delta^{13}C$ varying from 0‰ to –10‰ (Fig. 15). There is general agreement that peridotitic diamonds formed in the lithospheric mantle from carbon species derived from the upper mantle. The origin of the eclogitic diamond, however, is more controversial. The principal debate is whether the variable $\delta^{13}C$ values displayed by eclogitic diamonds are a consequence of biospheric input through subduction of the oceanic lithosphere (Kesson and Ringwood, 1989; Kirkley et al., 1991; Nisbet et al., 1994) or is due to primordial mantle heterogeneity (Deines et al., 1993) or high-temperature isotopic fractionation of carbon in the mantle (Javoy et al., 1986; Galimov, 1991).

Isotopic ratios of nitrogen in diamond are also important geochemical data that can constrain the origin of the diamond, particularly in combination with carbon isotopes. As pointed out by Cartigny et al. (1998), nitrogen is a useful tracer for sediments, because it is initially associated only with organic matter as a result of biological fixation. Since the Archean, organic matter has had positive $\delta^{15}N$ values. In contrast to these observations, all of the $\delta^{15}N$ values of diamonds in this study are negative, ranging from –2.8‰ to –15.8‰. Diamonds from Jwaneng, China (eclogitic type) and No. 50, China (peridotitic type) also have negative $\delta^{15}N$ (Cartigny et al., 1997, 1998). Additionally, if eclogitic diamonds are formed from recycled material, a correlation between the ratios of $\delta^{13}C$ and $\delta^{15}N$ should exist. It is expected that lower $\delta^{13}C$ will be accompanied by higher $\delta^{15}N$. However, in the U51 diamonds, despite very large variations of $\delta^{15}N$, the ratio of $\delta^{13}C$ remains almost constant at –5‰ (Fig. 15). The lack of a correlation between these ratios is consistent with the eclogitic diamonds from the Jwaneng pipe, and appears to support the argument that eclogitic diamonds are not formed from recy-

cled components (Cartigny et al., 1998). In order to explain the $\delta^{13}C$ and $\delta^{15}N$ values of our diamonds by recycling, it would be necessary to appeal to large isotopic fractionations or severe isotopic disequilibrium during growth, mechanisms that are at odds with the limited variability of $\delta^{13}C$ within each of the four studied diamonds.

As shown in Figure 15, eclogitic diamonds from the Jwaneng pipe exhibit a large variation of $\delta^{13}C$, but only a limited range for $\delta^{15}N$. However, contradictory features were observed in U51 eclogitic diamonds, which are comparable to peridotitic diamonds from the No. 50 pipe in China (Cartigny et al., 1998). This similarity may indicate that the CO_2-rich fluid/melt, from which the diamonds precipitated, could be of mantle origin. However, in order to explain the variability in $\delta^{15}N$, one needs to appeal to mechanisms such as variable fluid N isotope compositions, high-temperature N isotope fractionation, or kinetic isotope disequilibrium during incorporation into growing diamond (Hauri et al., 1999). There is no evidence in the present data that would serve to distinguish among these possibilities.

An Outrageous Hypothesis for Diamonds in the U51 Eclogite

The power of an outrageous hypothesis (Davis, 1926) lies in the stimulation that it generates within the scientific community. Some persons can remember their initial reactions to such concepts as "continental drift," "astroblemes," "Martian meteorites," and the "meteorite extinction of dinosaurs." This is not to suggest that what is presented below is of such caliber, but the following is certainly worthy of consideration.

As shown by the inclusions in the diamonds of this small eclogite, it would take a complex series of events in order to explain this rock and its minerals. However, we bring into question whether the diamonds were always in their present positions relative to each other. *We suggest that this eclogite xenolith is but the last residence place for these diamonds.* That is, *they may be relicts from other eclogite domains.*

It is obvious that there are large differences in the physical properties (e.g., Reynolds number) between diamond and Cpx and Gt. At the pressures (>4 GPa) and temperatures (>1000°C) prevalent in the upper mantle, diamond acts as a rigid solid, whereas Cpx and Gt behave plastically. With the plastic movement of eclogitic minerals in the mantle

and the resistant firmness of diamonds, it is possible that the diamonds might be presented with several new environments as they move among the eclogites. It is envisaged that the distances that the diamonds traverse may not be large, but movement of only tens of cm could bring the diamond in contact with considerably different eclogitic (or peridotitic) chemistry. Combine this with the effects of ever-present metasomatic fluids, and it is possible that a given diamond, over its growing lifespan, could be exposed to many different Cpx minerals to incorporate into its crystals. Lastly, the final spatial array of the diamonds may be locked in at lower temperatures, where the host eclogite finally homogenizes.

Conclusions

Variation in inclusion compositions in and between the diamonds in the U51 eclogite xenolith requires extreme changes in chemical environments during diamond growth. This is consistent with a metasomatic growth model for diamond (Kopylova et al., 1997; Stachel and Harris, 1997; Sobolev et al., 1998a, 1998b; Stachel et al., 1998; Taylor et al., 1998; Keller et al., 1999). Several significant conclusions have resulted from the present investigation.

1. The success of HRXCT at imaging diamonds within a mantle xenolith has several distinct benefits, both economic and scientific, as demonstrated in this study.

2. Thirty (30) macrodiamonds ($\geq$1 mm) appear to be associated with zones of secondary alteration in the xenolith, including partial melting of the primary Cpx.

3. The inclusions in the diamonds vary considerably in major- and trace-element chemistry within and between diamonds and do not correspond to the minerals of the host eclogite, whose compositions are extremely homogeneous. Some Cpx inclusions contain +Eu anomalies, probably inherited from their crustal components. The only consistent feature for the Cpxs in the inclusions is the presence of higher K_2O contents than that of the host Cpx.

4. The d^{13}C values are relatively constant at -5 ‰ both within and between diamonds, whereas $\delta^{15}N$ vary from -2.8 to -15.8‰. Within a diamond, the total N varies considerably from 15 to 285 ppm in one diamond, to 103 to 1250 ppm in another. CL imaging reveals extremely contorted zonations and complex growth histories in the diamonds, indicat-

ing very different growth environments for each diamond.

5. This study directly bears on the concept of diamond inclusions as time capsules for investigating the mantle of the Earth. The large variations in chemistry of inclusions within diamonds in the small U51 xenolith poses a serious question for all investigations of diamond inclusions.

Acknowledgments

REFERENCES

Boyd, F. R., and Finnerty, A. A., 1980, Conditions of origin of natural diamonds of peridotitic affinity: Jour. Geophys. Res., v. 85, p. 6911–6918.

Boyd, F. R., Pokhilenko, N. P., Pearson, D. G., Mertzman, S. A., Sobolev, N. V., and Finger, L. W., 1997, Composition of the Siberian cratonic mantle: Evidence from Udachnaya peridotite xenoliths: Contrib. Mineral. Petrol., v. 128, p. 228–246.

Bulanova, G. P., 1995, The formation of diamond: Jour. Geochem. Explorat., v. 53, p. 1–23.

Bulanova, G. P., Griffin, W. L., and Ryan, C. G., 1998, Nucleation environment of diamonds from Yakutian kimberlites: Mineral. Mag., v. 62, p. 409–419.

Carlson, W. D., and Denison, C., 1992, Mechanisms of porphyroblast crystallization: Results from high-resolution computed x-ray tomography: Science, v. 257, p. 1236–1239.

Carlson, W. D., Denison, C., and Ketcham, R. A., 1995, Controls on the nucleation and growth of porphyroblasts: Kinetics from natural textures and numerical models: Geol. Jour., v. 30, p. 207–225.

Cartigny, P., Harris, J. W., and Javoy, M., 1997, Eclogitic diamond formation at Jwaneng: No room for a recycled component: Nature, v. 280, p. 1421–1423.

Cartigny, P., Harris, J. W., Phillips, D., Girard, M., and Javoy, M., 1998, Subduction-related diamonds? — the evidence for a mantle-derived origin from coupled $\delta^{13}C$–$\delta^{15}N$ determinations: Chem. Geol., v. 147, p. 147–159.

Davis, W. M., 1926, The value of outrageous geological hypotheses: Fort Hays Series, Sc. Series, no. 63, p. 463–468.

Deines, P., and Harris, J. W., 1994, On the importance of fluids for diamond growth [ext. abs.]: Proc. Goldschmidt Ann. Geochem. Conference, Edinburgh, p. 219–220.

―――, 1995, Sulfide inclusion chemistry and carbon isotopes of African diamonds: Geochim. et Cosmochim. Acta, v. 59, p. 3173–3188.

Deines, P., Harris, J. W., and Gurney, J. J., 1993, Depth-related carbon isotope and nitrogen concentration variability in the mantle below the Orapa kimberlite, Botswana, Africa: Geochim. et Cosmochim. Acta, v. 57, p. 2781–2796.

Denison, C., and Carlson, W. D., 1997, Three-dimensional quantitative textural analysis of metamorphic rocks using high-resolution computed X-ray tomography: Part II. Application to natural samples: Jour. Metamor. Geol., v. 15, p. 45–57.

Denison, C., Carlson, W. D., and Ketcham, R. A., 1997, Three-dimensional quantitative textural analysis of metamorphic rocks using high-resolution computed X-ray tomography: Part I. Methods and techniques: Jour. Metamor. Geol., v. 15, p. 29–44.

Ellis, D. J., and Green D. H., 1979, An experimental study of the effect of Ca upon garnet-clinopyroxene Fe-Mg exchange equilibria: Contrib. Mineral. Petrol., v. 71, p. 12–22.

Fung, A. T., and Haggerty, S. E., 1995, Petrography and mineral compositions of eclogites from the Koidu kimberlite complex, Sierra-Leone: Jour. Geophys. Res., v. 100, p. 20,451–20,473.

Galimov, E. M., 1991, Isotope fractionation related to kimberlite magmatism and diamond formation: Geochim. et Cosmochim. Acta, v. 55, p. 1697–1708.

Griffin, W. L., Jaques, A. L., Sie, S. H., Ryan, C. G., Cousens, D. R., and Suter, G. F., 1988, Conditions of diamond growth: A proton microprobe study of inclusions in West Australian diamonds: Contrib. Mineral. Petrol., v. 99, p. 143–158.

Griffin, W. L, Kaminsky, F. V., Ryan, C. G., O'Reilly, S. Y., Win, T. T., and Ilupin, I. P., 1996, Thermal state and composition of the lithospheric mantle beneath the Daldyn kimberlite field, Yakutia: Tectonophys., v. 262, p. 19–33.

Hall, A. E., and Smith, C. B., 1985, Lamproite diamonds: Are they different?, in Glover, J. E., and Harris, P. G., eds., Kimberlite occurrence and origin: A basis for conceptional models in exploration: Geol. Dept. & Univ. Exten., Univ. Western Australia, Publ. 8., p. 167–212.

Haggerty, S. E., 1986, Diamond genesis in a multiply-constrained model: Nature, v. 320, p. 34–38.

Harlow, G. E., and Veblen, D. R., 1991, Potassium in clinopyroxene inclusions from diamonds: Science, v. 251, p. 652–655.

Hauri, E. H., Pearson, D. G., Bulannova, G. P., and Milledge, H. J., 1999, Microscale variations in C and N isotopes within mantle diamonds revealed by SIMS, in Gurney, J. J., Gurney, J. L., Pascoe, M. D., and Richardson, S. H., eds., Proc. VII International Kimberlite Conference, v. 1, p. 341–347.

Hervig, R. L., Smith, J. V., Steele, I. M., Gurney, J. J., Meyer, H. O. A., and Harris, J. W., 1980, Diamonds: Minor elements in silicate inclusions. Pressure-temperature implications: Jour. Geophys. Res., v. 85, p. 6919–6929.

Ireland, T. R., Rudnick, R. L., and Spetsius, Z., 1994, Trace elements in diamond inclusions from eclogites reveal link to Archean granites: Earth Planet. Sci. Lett., v. 128, p. 199–213.

Javoy, M., Pineau, F., and Delorme, H., 1986, Carbon and nitrogen isotopes in the mantle: Chem. Geol., v. 57, p. 41–62.

Jerde, E. A., Taylor, L. A., Crozaz, G., Sobolev, N. V., and Sobolev, V. N., 1993, Diamondiferous eclogites from Yakutia, Siberia: Evidence for a diversity of protoliths: Contrib. Mineral. Petrol., v. 114, p. 189–202.

Keller, R. A., Taylor, L. A., Snyder, G. A., Sobolev, V. N., Carlson, W. D., and Sobolev, N. V., 1999, Detailed pull-apart of a diamondiferous eclogite xenolith: Implications for mantle processes during diamond genesis, in Gurney, J. J., Gurney, J. L., Pascoe, M. D., and Richardson, S. H., eds., Proc. VII International Kimberlite Conference, v. 1, p. 397–412.

Kesson, S. E., and Ringwood, A. E., 1989, Slab-mantle interactionss: 2. The formation of diamonds: Chem. Geol., v. 78, p. 97–118.

Kirkley, M. B., Gurney, J. J., Otter, M. L., Hill, S. J., and Daniels, L. R., 1991, The application of C in diamonds: A review: Appl. Geochem., v. 6, p. 447–494.

Kopylova, M. G., Gurney, J. J., and Daniels, L. R. M., 1997, Mineral inclusions in diamonds from the River Ranch kimberlite, Zimbabwe: Contrib. Mineral. Petrol., v. 129, p. 366–384.

Mendelssohn, M. J., and Milledge, H. J., 1995, Geologically significant information from routine analysis of the mid-infrared spectra of diamonds: INT. GEOL. REV., v. 37, p. 95–110.

Meyer, H. O. A., 1968, Chrome pyrope: An inclusion in natural diamond: Science, v. 160, p. 1446–1447.

―――, 1987, Inclusions in diamonds, in Nixon, P. H., ed., Mantle xenoliths: Chichester, UK, Wiley, p. 501–523.

Meyer, H. O. A., and Boyd, F. R., 1968, Inclusions in diamonds: Yearbook Carnegie Inst. Washington, Yb66, p. 446–450.

Moore, R. O., and Gurney, J. J., 1989, Mineral inclusions in diamond from the Monastery kimberlite, South Africa, in Ross, J., ed., Kimberlites and related rocks: Geol. Soc. Austral. Publ. no. 14, p. 1029–1041.

Nisbet, D. E. G., Mattey, D. P., and Lowry, D., 1994, Can diamonds be dead bacteria?: Nature, v. 367, p. 694.

Otter, M. L., and Gurney, J. J., 1989, Mineral inclusions in diamond from the Sloan diatremes, Colorado-Wyoming State line kimberlite district, North America, *in* Ross, J., ed., Kimberlties and related rocks: Geol. Soc. Austral. Publ. no. 14, p. 1042–1053.

Pearson, D. G., Shirey, S. B., Bulanova, G. P., Carlson, R., and Milledge, H. J., 1999, Dating and paragenetic distinction of diamonds using the Re-Os isotope system: Application to some Siberian diamonds, *in* Gurney, J. J., Gurney, J. L., Pascoe, M. D., and Richardson, S. H., eds., Proc. VII International Kimberlite Conference, v. 2, p. 637–643.

Pearson, D. G., Snyder, G. A., Shirey, S. B., Taylor, L. A., Carlson, R. W., and Sobolev, N. V., 1995, Archean Re-Os age for Siberian eclogites and constraints on Archean tectonics: Nature, v. 374, p. 711–713.

Prinz, M., Manson, D. V., Hlava, P. F., and Kiel, K., 1975, Inclusions in diamonds: Garnet lherzolite and eclogite assemblages: Phys. Chem. Earth, v. 9, p. 797–815.

Richardson, S. H., 1986, Latter-day origin of diamonds of eclogitic paragenesis: Nature, v. 322, p. 623–626.

Richardson, S. H., Erlank, A. J., Harris, J. W., and Hart, S. R., 1990, Eclogitic diamonds of Proterozoic age from Cretaceous kimberlites: Nature, v. 346, p. 54–56.

Richardson, S. H., Gurney, J. J., Erlank, A. J., and Harris, J. W., 1984, Origin of diamond from old continental mantle: Nature, v. 310, p. 198–202.

Richardson, S. H., and Harris, J. W., 1997, Antiquity of peridotitic diamonds from the Siberian craton: Earth Planet. Sci. Lett., v. 151, p. 271–277.

Richardson, S. H., Harris, J. W., and Gurney, J. J., 1993, Three generations of diamond from old continental mantle: Nature, v. 366, p. 256–258.

Rowe, T., Kappelman, J., Carlson, W. D., Ketcham, R. A., and Denison, C., 1997, High-resolution computed tomography: A breakthrough technology for earth scientists: Geotimes, Sept., p. 23–27.

Schulze, D. J., Wiese, D., and Steude, J., 1996, Abundance and distribution of diamonds in eclogite revealed by volume visualization of CT X-ray scans: Jour. Geol., v. 104, p. 109–114.

Snyder, G. A., Taylor, L. A., Crozaz, G., Halliday, A. N., Beard, B. L., Sobolev, V. N., and Sobolev, N. V., 1997, The origins of Yakutian eclogite xenoliths: Jour. Petrol., v. 38, p. 85–113.

Snyder, G. A., Taylor, L. A., Jerde, E. A., Clayton, R. N., Mayeda, T. K., Deines, P., Rossman, G. R., and Sobolev, N. V., 1995, Archean mantle heterogeneity and the origin of diamondiferous eclogites, Siberia: Evidence from stable isotopes and hydroxyl in garnet: Amer. Mineral., v. 80, p. 799–809.

Snyder, G. A., Taylor, L. A., Keller, R. A., McCandless, T. E., Ruiz, J., and Sobolev, N. V., 1998, First internal Re-Os isochron for a diamondiferous eclogite, Yakutia, and evidence of Archean subduction of seafloor hydrothermal vent deposits [abs.]: EOS (Trans. Amer. Geophys. Union), v. 79, p. F1018.

Sobolev, N.V., Bakumenko, I. T., Yefimova, E. S., and Pokhilenko, N. P., 1991, Morphological features of microdiamonds, sodium in garnets, and potassium contents in clinopyroxene of two xenoliths from the Udachnaya kimberlite pipe (Yakutia): Dokl. Akad. Nauk SSR, v. 321, p. 585–591 (in Russian).

Sobolev, N. V., Snyder, G. A., Taylor, L. A., Keller, R. A., Yefimova, E. S., Sobolev, V. N., and Shimizu, N., 1998a, Extreme chemical diversity in the mantle during eclogitic diamond formation: Evidence from 35 garnet and 5 pyroxene inclusions in a single diamond: INT. GEOL. REV., v. 40, p. 222–230.

Sobolev, N. V., Taylor, L. A., Zuev, V. M., Bezborodov, S. M., Snyder, G. A., Sobolev, V. N., and Yefimova, E. S., 1998b, The specific features of eclogitic paragenesis of diamonds from Mir and Udachnaya kimberlite pipes (Yakutia): Russian Geol. Geophys., Geologiya i Geofizika, v. 39, no. 12, p. 1667–1678.

Sobolev, N. V., Yefimova, E. S., and Usova, L. V., 1983, Eclogitic paragenesis of diamonds from the Mir kimberlite pipe, *in* Mantle xenoliths and problems of ultrabasic magmas: Novosibirsk, Akad. Nauk SSR, Siberian Branch (in Russian).

Sobolev, V. N., Taylor, L. A., Snyder, G. A., and Sobolev, N. V., 1994, Diamondiferous eclogites from the Udachnaya kimberlite pipe, Yakutia: INT. GEOL. REV., v. 36, p. 42–64.

Sobolev, V. S., Sobolev, N. V., and Lavrent'yev, Y. G., 1972, Inclusions in diamonds from a diamond-bearing eclogite: Dokl. Akad. Nauk. SSSR, v. 207, p. 164–167 (in Russian).

Spetsius, Z. V., 1995, Diamondiferous eclogites from Yakutia: Evidence for a late and multistage formation of diamonds [abs.]: VI International Kimberlite Conference, Novosibirsk, p. 572–574.

Spetsius, Z. V., and Griffin, B. J., 1998, Secondary phases associated with diamonds in eclogites from the Udachnaya kimberlite pipe: Implications for diamond genesis [abs.]: VII International Kimberlite Conference, Cape Town, p. 850–851.

Spetsius, Z. V., and Taylor, L. A., 2001, Partial melting of clinopyroxene in diamondiferous eclogite xenoliths: INT. GEOL. REV., submitted.

Stachel, T., and Harris, J. W., 1997, Diamond precipitation and mantle metasomatism—evidence from the trace element chemistry of silicate inclusions in diamonds from Akwatia (Ghana): Contrib. Mineral. Petrol., v. 129, p. 143–154.

Stachel, T., Harris, J. W., and Brey, G., 1998, Inclusions in diamonds from Mwadui (Tanzania)—chemical mush in the source [abs.]: VII International Kimberlite Conference, Cape Town, p. 859–861.

Taylor, L. A., 1993, Evolution of the subcontinental mantle beneath the Kaapvaal craton: A review of evidence for crustal subduction for Bellsbank eclogites: Russian Geol. Geophys., Geologiya i Geofizika, v. 34, no. 12, p. 21–39.

Taylor, L. A., Milledge, H. J., Bulanova, G. P., Snyder, G. A., and Keller, R. A., 1998, Metasomatic eclogitic diamond growth: Evidence from multiple diamond inclusions: INT. GEOL. REV., v. 40, p. 592–604.

Taylor, L. A., and Neal, C. R., 1989, Eclogites with oceanic crustal and mantle signatures from the Bellsbank kimberlite, South Africa, Part I: Mineralogy, petrography, and whole rock chemistry: Jour. Geol., v. 97, p. 551–567.

Taylor, L. A., Snyder, G. A., and Camacho, A., 1999, Diamond: Just another metamorphic mineral [abs.]?: Proc. Goldschmidt Ann. Geochem. Conf., p. 66–67.

Taylor, L. A., Snyder, G. A., Crozaz, G., Sobolev, V. N., and Sobolev, N. V., 1996, Eclogitic inclusions in diamonds: Evidence of complex mantle processes over time: Earth Planet. Sci. Lett., v. 142, p. 535–551.

Taylor, W. R., Jaques, A. L., and Ridd, M., 1990, Nitrogen-defect aggregation characteristics of some Australasian diamonds: Time-temperature constraints on the source regions of pipe and alluvial diamonds: Amer. Mineral., v. 75, p. 1290–1310.

Wang, W., 1998, Formation of diamond with mineral inclusions of "mixed" eclogite and peridotite paragenesis: Earth Planet. Sci. Lett., v. 160, p. 831–843.

Yurimoto, H., Yamashita, A., Nishida, N., and Sueno, S., 1989, Quantitative SIMS analysis of GSJ rock reference samples: Geochem. Jour., v. 23, p. 215–236.